

Oscillatory modes of concentration convection

M O Denisova, A L Zuev, K G Kostarev

DOI: <https://doi.org/10.3367/UFNe.2021.07.039030>

Contents

1. Introduction	767
1.1 Capillary phenomena: a history of observations and research; 1.2 Specifics of the development of solutocapillary convection; 1.3 Observation of oscillatory regimes of Marangoni convection	
2. Oscillating flow near immobile bubbles and drops in stratified surfactant solutions	771
2.1 Concentration flow around a bubble in a two-layer system of liquids; 2.2 Bubble in a vertical layer of a stratified surfactant solution; 2.3 Mass transfer between a drop and an inhomogeneous surfactant solution (vertical layer); 2.4 Mass transfer between a drop and an inhomogeneous surfactant solution (horizontal layer)	
3. Oscillatory regimes of concentration convection in a horizontal channel	780
3.1 Threshold development of Marangoni convection near bubbles and drops with a vertical interface; 3.2 Effect of surfactant surface activity on the period of oscillations	
4. Laboratory simulation of Marangoni convection in microgravity	783
4.1 Oscillatory regimes of convective flow in a drop connected to a container; 4.2 Simulation of Marangoni instability for homogeneous diffusion of surfactants through an interface under zero-gravity conditions	
5. Conclusions	786
References	787

Abstract. Experimental studies of oscillatory regimes of Marangoni concentration (solutal) convection, which are due to competition between the capillary and gravitational mechanisms of motion in two-phase fluid systems, are reviewed. Application of optical methods enables advancement from a qualitative description of phenomena to quantitative measurements; it also makes it possible to determine the oscillation period and duration of the oscillatory mode as functions of the features of the concentration distribution of surfactants, physicochemical properties of contacting fluids and the surfactants employed, and the surface activity of the surfactants. The development of oscillatory flow regimes in the vicinity of bubbles and drops in vertical and horizontal layers and near vertical phase interfaces is analyzed.

Keywords: Marangoni convection, solutocapillary flows, surface tension, phase interface, oscillation regime

1. Introduction

1.1 Capillary phenomena: a history of observations and research

The nature of the movement of a liquid with a phase interface is in most cases determined by the concurrent action of bulk and surface forces [1]. Of the bulk forces, the most famous is the Archimedes force, which occurs due to a local change in the density of a liquid in a gravitational field; of surface forces, it is capillary forces, which are due to the inhomogeneous distribution of surface tension at the interface. The value of surface tension σ is determined by the energy difference between the interaction of liquid molecules with each other and with molecules of the contacting phase. As a result, σ depends on the temperature T of the liquid and the pressure of the gas (vapor) above it: with an increase in these parameters, σ decreases until vanishing when the critical temperature T_{cr} is reached. The surface tension is also affected by the composition of the liquid (if it consists of several components). The molecules of one of the components of a liquid usually have a lower interaction energy; therefore, it is advantageous for a liquid to have these molecules at the interface with another phase. The predominance of such molecules is only observed on the surface of the liquid and in the near-surface layer, since the intermolecular forces are short range and rapidly decrease with increasing distance [2]. Liquids, as well as solid and gaseous substances that reduce the surface tension of a liquid system in the dissolved state, are currently combined into a large group of surface-active substances (surfactants). In addition, the value of surface tension is affected by an external electric field; however, the main interest is focused on the dependence of σ on temperature and concentration.

M O Denisova^(1,a), A L Zuev^(1,2,b), K G Kostarev^(1,c)

⁽¹⁾ Perm Federal Research Center,

Ural Branch of the Russian Academy of Sciences,
ul. Akademika Koroleva 1, 614013 Perm, Russian Federation

⁽²⁾ Perm National Research Polytechnic University,

Komsomol'skii prosp. 29, 614990 Perm, Russian Federation

E-mail: ^(a) mod@icmm.ru, ^(b) zal@icmm.ru, ^(c) kostarev@icmm.ru

Received 9 April 2021, revised 26 July 2021

Uspekhi Fizicheskikh Nauk 192 (8) 817–840 (2022)

Translated by M Zh Shmatikov

Historically, capillary phenomena caused by the action of surfactants were the first to attract attention. For example, even Plutarch and Pliny the Elder tried to find out the reason for the sharp decrease in the height of waves when olive oil was poured onto the surface of the sea during a storm [3]. The ‘unpredictable’ movement of islets of soap foam over the water surface, ‘legs’ on the inside of a wine glass, and many other phenomena associated with the manifestation of capillary forces also gained wide popularity long before the start of a dedicated study of the movement of a liquid surface as an independent object. Apparently, the description of motion in evaporating drops (C Varley [4], 1836) and convective flows on the surface of bubbles in alcohol solutions (E Weber [5], 1854) were the first experimental studies of capillary effects. In 1855, James Thomson (Lord Kelvin’s elder brother) made an attempt to explain the phenomenon of the formation of ‘wine legs’ in a glass of strong alcohol solution (Thomson effect) by the movement of the liquid surface when surface tension gradients arise due to a difference in concentration inside the solution [6]. It should be noted that the very concept of surface tension was introduced by J Segner in 1751 by analogy with membrane tension in the theory of elasticity [7]. However, Carlo Marangoni, who experimentally studied the spreading of one liquid over the surface of another in vessels with different surface areas, is considered to be the founder of the science of fluid flow along an interface. He was the first to note that a fluid begins flowing towards the region of greater surface tension. Marangoni first reported this phenomenon in 1865 in a small pamphlet [8], in a hurry for fear of losing priority in connection with the work of the Belgian researcher G Van der Mensbrugghe [9, 10] (1870, 1873). Marangoni presented the results of his research in a more accessible form a few years later [11, 12] (1870–1871). J Plateau in his book [13] published in 1873 paid tribute to the work of Marangoni, recognizing its priority, and described the work of Dupré de Rennes [14], finding in the latter quite a lot of similarities with Marangoni’s experiments.

Undoubtedly, one of the incentives for setting up these experiments was the development of the theory of capillary phenomena by T Young [15] (1805) and P Laplace [16] (1806). The experimental results, in turn, served as the basis for the theoretical work of J Maxwell [17] (1871), [18] (1878) and, later, W Harkins and A Feldman [19] (1922). The thermodynamic theory of capillary phenomena published by J Gibbs [20, 21] in 1878 was a big step forward. He introduced the concepts of the interface between contacting media as an independent phase and the characteristics inherent to this phase alone (concentration, viscosity, etc.), the magnitudes of which differ from similar volumetric ones. These concepts made it possible to describe the properties and dynamics of the behavior of the surface. At the same time, a concise presentation of the main provisions of the theory gave rise to numerous discussions among contemporaries and triggered the development of its individual sections in much later studies by A N Frumkin [22] (1928), J Rice [23] (1936), V G Levich [3] (1959), F Buff [24] (1951), S Kondo [25] (1956), P Rebinder [26] (1978), and A I Rusanova [27, 28] (1960, 1967).

The revival of active interest in capillary effects at the beginning of the 1950s can be associated with the publication by J Lewis and H Pratt, who reported the results of their observations of the behavior of a drop of a mixture of carbon tetrachloride and acetic acid dissolved in water. In an attempt to determine the value of surface tension, they noticed that

when a certain concentration of acid in a drop was reached, the latter began to swing intensively and unpredictably on a suspension [29] (1953). In describing this movement of a drop, Lewis and Pratt associated it with the instability of the drop surface due to the emergence of local surface tension inhomogeneities during acid dissolution. A theoretical description of the observed phenomenon was provided by V Sterling [30] (1959) and L Scriven [31] (1960), and for the thermal case, by N Young, J Goldstein, and M Block [32] (1959). It should be noted that these studies are usually cited as conceptual, the emergence of which rekindled interest in capillary phenomena, while leaving the Lewis and Pratt experiment in oblivion.

The resumption of active research on capillary flows was also due to the advent of the space exploration era. Capillary convection turned out to be the only mechanism of fluid motion known at that time which retains its effect when gravity and, accordingly, the Archimedes force disappear [2, 33–36]. Active interest in the motion of a fluid under the action of surface forces, especially in the absence of gravity, is observed even now. It would be sufficient to point out that hundreds of thousands of studies devoted to hydrodynamics and heat and mass transfer involving Marangoni effects have been published, and the number of links offered by the Google search engine to the phrase ‘Marangoni convection’ exceeds a million. A significant part of the work on the study of Marangoni convection has already been systematized in a number of popular reviews and monographs [37–47], thematic collections of articles and conference proceedings, including the International Association for the Study of Marangoni Convection (International Marangoni Association (IMA) conferences: Gießen (2001), Brussels (2004), Gainesville (2006), Tokyo (2008), Florence (2010), Haifa (2012), Vienna (2014), Bad Honnef (2016), and Guilin (2018)).

1.2 Specifics of the development of solutocapillary convection

This review is devoted to the study of oscillatory regimes of concentration convection due to the presence of a nonuniform concentration C of surfactants over the phase interface. Similar to the case of thermocapillary convection due to the inhomogeneity of the surface temperature, the emerging tangential capillary force initiates the surface flow in the direction of increasing surface tension. The intensity of such a flow is determined by the dimensionless Marangoni number, which characterizes the ratio of the forces of surface tension and viscous dissipation.

The thermal Marangoni number is determined by the formula $Ma_T = h^2 \sigma_T' \nabla T / (\eta \chi)$, and the concentration number $Ma_C = h^2 \sigma_C' \nabla C / (\eta D)$, where h is the characteristic size, η is the dynamic viscosity, χ is the thermal diffusivity, D is diffusion coefficient, and $\sigma_T' = \partial \sigma / \partial T$ and $\sigma_C' = \partial \sigma / \partial C$ are, respectively, the temperature and concentration coefficient of surface tension.

The presence of temperature or concentration gradients along the surface and, consequently, in the volume of liquid itself, in turn, inevitably gives rise to local density inhomogeneities, which also depend on temperature and concentration. As a result, Rayleigh gravitational convection concurrently develops in a liquid medium, the intensity of which under terrestrial conditions often turns out to be several ten or even several hundred times higher than that of Marangoni convection. The latter thus turns out to be almost completely suppressed by a more powerful convective mechanism (if the

directions of capillary and gravitational flows are opposite) or masked by its action. The intensity of gravitational convection and other phenomena associated with the action of gravity can be significantly suppressed under conditions of a terrestrial laboratory by reducing the characteristic vertical size of the liquid volume. The situation in which surface forces are sufficiently large compared to volume forces is realized, for example, in thin layers and films of a liquid, liquid bridges and zones enclosed between solid surfaces, and small insoluble drops or gas bubbles suspended in a liquid. Since the intensity of thermogravitational convection is determined by the Rayleigh number, which characterizes the ratio of thermogravitational forces to viscous friction forces, expressed as $Ra = \rho g \beta_T h^4 \nabla T / (\eta \chi)$ (here, g is gravity acceleration, ρ is the density of the liquid, and β_T is the coefficient of volumetric thermal expansion), for the predominance of the thermal capillary mechanism over the gravitational one, the value $Bd = Ra/Ma_T = \rho g \beta_T h^2 / \sigma'_T$, which is called the dynamic Bond number, should be less than one. This condition limits the thickness of liquid layers and films (or the vertical size of liquid zones, droplets, and bubbles) used to study thermocapillary phenomena under normal gravity. In particular, for an ethanol layer, the critical thickness $h^* = [\sigma'_T / (\rho g \beta_T)]^{1/2}$, for which $Bd = 1$, is about 3 mm.

It should be noted that, along with the Rayleigh number, the Grashof number $Gr = Ra/Pr$ is often used, where $Pr = \eta / (\rho \chi)$ is the Prandtl number, which describes the ratio of the viscous and thermal dissipative characteristics of the liquid. Its concentration analog is the Schmidt number $Sc = \eta / (\rho D)$. Rayleigh numbers are usually used in stability problems, while Grashof numbers are used to characterize steady-state flows.

Although thermocapillary phenomena turned out to be studied much better due to the relative simplicity of creating and maintaining a temperature difference in the volume and on the surface of a liquid, solutocapillary analogs are more intense. For example, the difference in surface tension that occurs when a drop of ethyl alcohol is placed on the surface of water reaches almost 51 dyn cm^{-1} , while local heating of water from 0°C to 95°C leads to the formation of a difference in σ of 15 dyn cm^{-1} . Taking into account that the diffusion coefficients in liquids are usually 2–3 orders of magnitude smaller than the thermal conductivity coefficients, the Schmidt numbers and the concentration (diffusion) Marangoni Ma_C numbers usually turn out to be significantly larger than the thermal ones (for the above case, $Ma_C/Ma_T \sim 10^2$). Consequently, it may be expected that solutocapillary effects are exhibited in liquid volumes with a larger vertical size. The small value of the diffusion coefficient also leads to the concentration inhomogeneities of the density in the liquid existing much longer than the thermal ones, and their value is often greater than the thermal variant (in the case considered above with the introduction of a drop of alcohol and local heating of water, $\Delta\rho_C \sim 0.2 \text{ g cm}^{-3}$ and $\Delta\rho_T \sim 0.03 \text{ g cm}^{-3}$, respectively).

In addition, surfactant adsorption on the interface, which is absent in the thermal case, plays an additional role. Indeed, the surface of a liquid cannot spontaneously heat up by means of cooling the rest of the volume of the liquid to lower the surface energy of the entire system, since this is forbidden by the laws of thermodynamics. However, the situation in which the same surface adsorbs on itself molecules of a substance with a low surface tension, extracting them from the rest of the solution, is quite energetically advantageous and possible.

In general, the mechanism of surfactant release to (adsorption on) the phase interface differs from the mechanism of formation of the boundary temperature, since the interface has inertial properties, and convective transfer of surfactant along the interface and its surface diffusion are possible.

Two more differences need to be pointed out. First, the liquid surface can adsorb not only surfactants whose composition and concentration are known in the experiment, but also residual impurities of the working liquid, whose surface tension is lower than that of the liquid, and the substances coming from the contacting (gas or liquid) phase in the form of individual molecules and insoluble particles (dust). A decrease in surface tension due to the emerging adsorbed film leads to a decrease in the intensity of Marangoni convection. In addition, in the case of a relatively slow creation of a surface tension gradient, adsorbed molecules and particles can be redistributed over the liquid surface, compensating its effect and thereby hindering the onset of capillary motion. Since neither the composition of such an adsorbed film nor the change in its state in hydrodynamic experiments is practically ever controlled, such adsorption is *a priori* considered the main mechanism leading to low reproducibility of results in the study of capillary phenomena in liquids with a high surface tension.

The occurrence of a temperature gradient along the liquid surface does not affect the concentration of uncontrolled surface-active impurities (USAIs). On the contrary, the introduction of surfactants, which are largely organic solvents, significantly changes both the composition and the concentration of USAI in the direction of decrease, increasing the likelihood of the emergence of Marangoni convection and its intensity. Another difference is related to the methodology of the experiment. Optical (contactless) methods are currently the most promising for studying the structure and evolution of temperature and concentration fields. The sensitivity of most of these methods is determined either by the difference in the refractive index, or by its gradient (respectively, interference and shadow methods). Since the refractive index is largely determined by the density of the medium, and the resulting density differences are higher in the concentration case, the latter seems to be more attractive for exploration. Another advantage of the concentration variant is the low diffusion coefficient of the mixture components, due to which the concentration field is ‘frozen’ into the moving volume of the liquid. This circumstance enables not only tracking the evolution of concentration distributions, but also revealing the structure of flows.

The main objects of our study are bubbles and drops in a surfactant gradient solution. There are two options for the behavior of these inclusions, depending on their degree of freedom. If the inclusion is able to move, the occurrence of a difference in interfacial tension along its surface sets the latter in motion in the direction of increasing tension. In this case, the inclusion itself begins to shift in the opposite direction (so-called thermal or solutocapillary drift [48, 49]). If the inclusion cannot move, the movement of its surface is transferred to the environment, leading to the formation of a cellular flow. The surface entrains the adjacent layers and takes them to an area with a lower temperature or surfactant concentration (and, consequently, with a different density). Having left the vicinity of the inclusion, these layers under the action of gravity return to the equal density level. It should be noted that, in the thermal variant, a liquid entrained by the surface, due to the relatively high thermal conductivity, has time to partially cool down. As a result, a difference in

temperature (and surface tension) continues to be maintained along the inclusion surface, although it is smaller than the initial one. Consequently, the emerging cellular motion, except for the case of very high temperature differences, acquires a stationary character.

In the concentration variant, the situation is somewhat different. In its motion, the interfacial surface not only entrains the boundary layers but also actively participates in mass exchange with them, absorbing the surfactant from the inflowing solution and partially returning it to the outgoing flow. The size of the emerging convective cell grows due to the involvement of the surrounding liquid in the movement, while, inside the cell itself, the concentration of the solution is levelled. As a result, the difference in interfacial tension along the surface is only maintained by a narrow jet of fresh solution, and, as soon as the growing cell blocks it, the capillary motion stops. The rotation of the cell slows down, and the fluid contained in it spreads along an equal-density plane, giving rise to an advective flow. Over time, this flow partially restores the surfactant concentration difference along the interfacial surface, leading to a new ‘burst’ of capillary convection. The cycle is repeated (see Section 2.2 for details).

1.3 Observation of oscillatory regimes of Marangoni convection

E Horn et al. was apparently the first study to describe the onset of such an oscillatory regime of capillary convection [50] (1978). In their study on electrochemistry, the passage of current through an inhomogeneous aqueous solution of sodium chloride was experimentally studied, where one of the electrodes was a drop of mercury immersed in the solution. Periodic fluctuations in the current amplitude were found, which the authors attributed to the occurrence of oscillating capillary convection in the solution due to a surface tension difference on the interfacial surface of the mercury drop. It should be noted that the periodic development of capillary convection could be detected even earlier, at certain stages of acid diffusion from a drop in the experiments of Lewis and Pratt described above. However, this required changing the direction of observation of the drop (from lateral to vertical), i.e., going beyond the study of the dynamics of changes in interfacial tension in the course of mass transfer processes.

The development of oscillatory modes of solutocapillary convection was also observed in other situations. For example, Mu Wang and Nai-ben Ming [51] (1991) described the growth of a single crystal on a substrate in a thin horizontal layer of an aqueous solution of a $\text{Ba}(\text{NO}_3)_2$ salt placed on a glass plate under isothermal conditions. As a result of the evaporation of water from the free surface, the solution turned out to be supersaturated, and a crystal began to grow in it in the form of a long thin needle. The authors found an oscillating behavior of the surface of this solution. The oscillatory flow in the liquid was explained by the development of solutocapillary deformation, which periodically pushes the salt solution layer away from the crystallization surface.

The onset of oscillatory modes due to evaporation is also described in a series of studies devoted to the management of ispalators (a Russian term proposed by Yu Yu Stoilov as a contraction of the words ‘evaporator’ and ‘oscillator’)—horizontal two-layer systems of liquids with stable discontinuity of the upper layer [52–54]. The lower continuous layer (substrate) is formed by a liquid with a higher density and a

lower value of surface tension than those of the upper liquid. The discontinuity has the form of a ring with an inner diameter that depends on the thickness of the upper layer, and it can be free or partially filled with a third liquid. All liquids are mutually insoluble and wet the cell walls. The conditions for the existence of such a discontinuity are described in [55]. Having the smallest value of σ , the lower layer liquid spreads over the upper layer in the form of a thin rapidly evaporating film. In cells of a relatively small diameter, the film has time to reach the cell walls and ascend along them, entraining with it the upper layer liquid (or the third liquid that filled the gap). Periodically—as they accumulate—these liquids flow down in the form of drops and a small-size film like ‘wine legs’ in a glass. The falling drops and the ascending film of the liquid-substrate form an unsteady cellular motion. A similar periodic motion can also be observed in the meniscus region of solutions that contain easily evaporating components [56].

Later, the existence of oscillatory regimes was also discovered in some thermal problems with Marangoni effects. It was shown in [57–65] that, in the presence of an upward temperature gradient in a liquid, a thermocapillary flow is formed around a gas bubble, which is pressed from below to a solid plane, in the form of an axisymmetric toroidal vortex with a vertical symmetry axis. The liquid, entrained by the Marangoni forces, is transported along the free surface of the bubble to its lower pole, and away from it slowly ascends, creating a return flow. Such a flow maintains its stability at values of the thermal Marangoni number up to $\text{Ma}_T \sim 3 \times 10^4$ [66], at which it loses symmetry and acquires an azimuthal velocity component. As a result, a weak and slow oscillation of the thermal field near the bubble develops in the horizontal direction [67]. The emergence of such an oscillatory mode, which does not depend on the force of gravity [68], is explained by the loss of stability of the laminar flow at high speeds of motion. Looking ahead, we note that similar oscillatory modes corresponding to the diffusion Marangoni numbers $\text{Ma}_C = 4.0 \times 10^4$ are realized in aqueous solutions of ethyl alcohol already at a concentration difference of $\Delta C \sim 0.1\%$ between the poles of bubbles of the same sizes, as in the thermal case. Since in the experiments the initial differences in the concentration of the dissolved surfactant are significantly higher, the onset of an oscillatory regime is usually observed first, which is followed by a transition to a monotonous flow at the end of the experiment.

Oscillating deformation of a free surface due to thermocapillary convection, but this time from a submerged heat source, was discovered in an experiment of A I Mizev (2004) [69]. It has been shown that, in the case of a deep container, the intensities of thermocapillary and thermogravitational convection can become comparable, which leads to oscillations of the free surface above the heater at a certain threshold value of its immersion depth. In this case, the configuration of the emerging surface waves depends on the distance from the surface and on the power of the heater. In particular, if the depth of immersion of the heat source is fairly large, surface waves have the shape of concentric circles. Reducing the depth of immersion leads to the formation of a spiral wave rotating to the right or left. The number of spiral wave branches increases as the distance to the surface decreases. If the heater touches the surface, wave oscillations halt, but a stationary standing wave ray-like structure is formed. It is shown that circular waves are characterized by a constant radial velocity of wave front propagation and wave number.

For spiral waves, the space-time dependence becomes non-linear. However, if the distance from the source increases further, the velocity and spatial frequency approach the values for a circular wave.

A concentration analog of the experiment considered above is the development of an oscillatory regime of capillary motion due to a submerged surfactant source [70, 71]. Surface tension fluctuations caused by the supply of portions of a weakly soluble surfactant from its submerged source to the free surface are studied. The ‘burst’ of the emerging capillary convection stops as the surfactant propagates along the free surface and is subsequently dissolved in the bulk of the liquid. Influence on the periodicity and intensity of ‘bursts’ of the capillary flow of the physical and chemical properties of surfactants and the liquid filling the container, the geometrical parameters of the setup, and the depth of the surfactant source are discussed. A detailed bibliography of a comprehensive study of this problem can be found in [72]. The hydrodynamic component of this problem was later explored experimentally and theoretically by Mizev and Birikh [73] (2011). The use of a vertical Hele-Shaw cell with a submerged surfactant source, along with the visualization of flows and concentration fields, made it possible to clarify the mechanisms for the formation of an oscillatory regime. It has been found that the competition between the gravitational and capillary mechanisms of motion leads to the onset of oscillations and, consequently, the period of the observed oscillations primarily depends on the balance between the Grashof and Marangoni numbers and on the ratio of the geometric parameters of the problem. It has been shown that, if the contribution of free convection increases, the oscillatory regime is replaced with the stationary one.

The work of K Eckert et al. [74] should be especially noted, which is devoted to the development of a neutralization reaction at a horizontal interface. The density and diffusion of the reaction product (salt of a carboxylic acid) differ from those of the ambient aqueous solution of the base, and it also exhibits surface-active properties with respect to it. All these factors result in a complex interaction between the gravitational, capillary, and diffusion mechanisms of mass transfer, which is manifested in the periodic alteration of intense cellular Marangoni convection and slow gravitational flow in the form of finger-like structures.

In concluding this review of the most significant studies of oscillatory modes of motion in systems of liquids with an interface, their common feature should be emphasized. The

overwhelming majority of them are devoted to purely three-dimensional objects. On the one hand, this allows identification of the entire spectrum of movements. On the other hand, the structure and evolution of the concentration and temperature fields have to be assessed based on boundary conditions and the observation of oscillations of one or two of the characteristics of the system (surface tension, surface deformation, the shape of the convective cell around the bubble, etc.). Based on the dependence obtained, a model of the phenomenon is suggested, which is based on Marangoni convection and some additional mechanism (an adsorption-desorption process, gravitational convection, heat diffusion, etc.). The adequacy of the model is verified by subsequent numerical simulation, usually two-dimensional, based on this model. However, this approach leaves many questions unanswered and allows an error to occur in choosing the additional mass transport mechanism.

2. Oscillating flow near immobile bubbles and drops in stratified surfactant solutions

The most promising way to solve the problems described above, in our opinion, is to advance to the exploration of such problems in a 2D formulation using Hele-Shaw cells, which enable visualization of temperature and concentration fields using the interference method. The results obtained can be further extended to the 3D case. In particular, in our experiments, we used a setup based on a Fizeau autocollimation interferometer (Fig. 1a) with one or two video cameras connected to a computer [75]. In some experiments, concurrently with video filming, the temperature was measured at the reference points of the liquid system using a differential thermocouple unit. The experimental cell was a Hele-Shaw cell located vertically or horizontally, depending on the task, in the form of a thin (1.2 mm thick) rectangular cavity 90×40 mm in size with walls made of plane-parallel glass with a semi-transparent mirror coating (Fig. 1b). The observation was carried out from the side of wide faces. If the cell was vertically oriented, the interferometer made it possible to visualize the inhomogeneities of the concentration/temperature distribution in the solution in the form of a system of isolines, which represent bands of equal optical paths. If the mixture composition only varied across the probing light beam, in the isothermal case, each interference fringe could be associated with a certain concentration of the dissolved substance, using the concentration dependence of

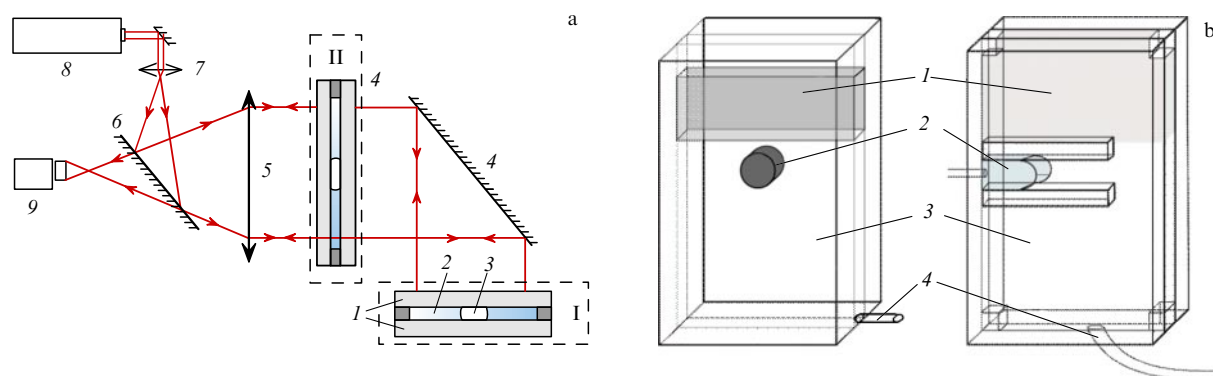


Figure 1. (Color online.) (a) Experimental setup: 1 — flat glass with a semi-transparent mirror coating; 2 — layer of liquid; 3 — air bubble; 4 — mirror; 5 — object lens; 6 — semi-transparent mirror; 7 — microobject lens; 8 — He-Ne laser; 9 — video camera. I, II — cell position for horizontal and vertical orientations. (b) Experimental cell: 1 — surfactant solution; 2 — bubble/drop; 3 — base fluid; 4 — tube for filling the cell.

the refractive index. With the horizontal orientation of the cell, the equal concentration isolines turned out to be parallel to the wide face, and the probing radiation beam passed through them perpendicularly. In this case, the optical path turned out to be the same for all parts of the probing beam, and the image of the cell was uniformly colored. The occurrence of local concentration inhomogeneity led to the emergence of a system of interference fringes. And although it was then impossible to correlate each fringe with a specific drop in concentration, it was still possible to estimate the horizontal size of the inhomogeneity and to trace its evolution.

2.1 Concentration flow around a bubble in a two-layer system of liquids

The onset of an oscillatory regime of concentration convection was discovered in an experiment on studying the solutocapillary drift of bubbles in a horizontal layer of a solution with a longitudinal surfactant gradient [48, 49]. To obtain such a gradient in a vertical Hele-Shaw cell, a two-layer system was created based on an aqueous solution of surfactants of different concentrations stratified in density in a stable form. Methyl, isopropyl, and ethyl alcohols (with a mass concentration of solution $C_0 = 40\text{--}100\%$) and acetic acid (with $C_0 = 0\text{--}70\%$) were used as surfactants. All selected surfactants are soluble in water without limitations. The density of acetic acid is higher and the density of alcohols is lower than that of water. This circumstance enables the creation of concentration gradients (and surface tension gradients) directed both up and down.

After creating a system of solutions separated by a diffusion zone, the cell was rotated to a horizontal position and layer-by-layer inflow with stirring occurred. After the longitudinal difference in concentration leveled, the cell was returned to the vertical position. It turned out that, as a result of these operations, the solutions were only partially mixed, so the concentration distribution reappeared in the vertical cell, with a significantly expanded diffusion zone but with the initial concentration difference. To create a longitudinal concentration gradient close to the stationary one, the described procedure had to be repeated several times. It was also found that, in a horizontal cell, around small bubbles that spontaneously appeared due to a decrease in the solubility of gases in a surfactant solution with a decrease in its concentration, a periodic short-term perturbation of the concentration field developed, the longitudinal dimensions of which significantly exceeded the diameter of the bubbles (Fig. 2). It was suggested that such a disturbance could be caused by Marangoni convection (due to the conservation of

the vertical gradient of the surfactant concentration). The convective motion quickly leveled the surfactant difference along the lateral surface of the bubble, after which it decayed for a sufficiently long time until the surfactant distribution was restored near the bubble.

For further study of the discovered phenomenon, the following technique was used [76]. The specified vertical difference in the surfactant concentration in a horizontal cell was created, as before, by rotating the vertical cell with a two-layer system of solutions to a horizontal position. An air bubble was then introduced into the cell using a medical syringe. The size of the bubble usually exceeded the cell thickness; therefore, it took the form of a flat disk 5–15 mm in diameter with a free lateral surface. Observations have shown that the evolution of the concentration field near the bubble could occur, depending on the initial drop in the surfactant concentration ΔC_0 , according to one of three scenarios. In particular, for a two-layer system consisting of distilled water and an aqueous solution of acetic acid with $\Delta C_0 < 15\%$, the concentration difference in the cell was leveled exclusively by diffusion. In the range $15 < \Delta C_0 < 60\%$, as some time elapsed after the bubble was introduced (Fig. 2a), a ‘burst’ of an intense but rapidly decaying motion occurred (Fig. 2b), after which a perturbation wave propagated from the bubble (Fig. 2c) followed by a long pause. This process was repeated over and over with fairly high regularity. The period T of such oscillations, defined as the time interval between two bursts of intense convection, ranged from a few seconds to several minutes and depended on the time from the moment the bubble was introduced, its horizontal diameter, the initial concentration difference, the average concentration of the solution, physical fluid properties, and layer thickness. At $\Delta C_0 > 60\%$, the oscillations were so frequent that they looked like ‘boiling’ of a saturated surfactant solution around the bubble. Over time, as the concentration difference in the cell decreased, the ‘boiling’ was replaced by the regime of separate ‘bursts’. It should be noted that for alcohol solutions the range of concentrations that drove oscillations was much narrower, and ‘boiling’ was the main mechanism of mass transfer.

Figure 3a shows the time change in the oscillation frequency in a two-layer system consisting of water and a 40% aqueous solution of acetic acid for bubbles with a diameter ranging from 2.4 to 15.0 mm. It can be seen that, as the solution was mixed and the vertical concentration gradient decreased, the period of oscillations, initially equal to 10 s, gradually increased (the frequency decreased accordingly) and the oscillations occurred increasingly less frequently, until they ended after about 10 minutes. The above



Figure 2. Evolution of the concentration field perturbation around an air bubble in a horizontal layer of an aqueous solution of isopropyl alcohol. Layer thickness $h = 2.6$ mm, concentration difference $\Delta C = 20\%$, bubble diameter $d = 5.0$ mm. Top view: (a) $t = 0$, (b) $t = 2.0$ s, (c) $t = 10.0$ s.

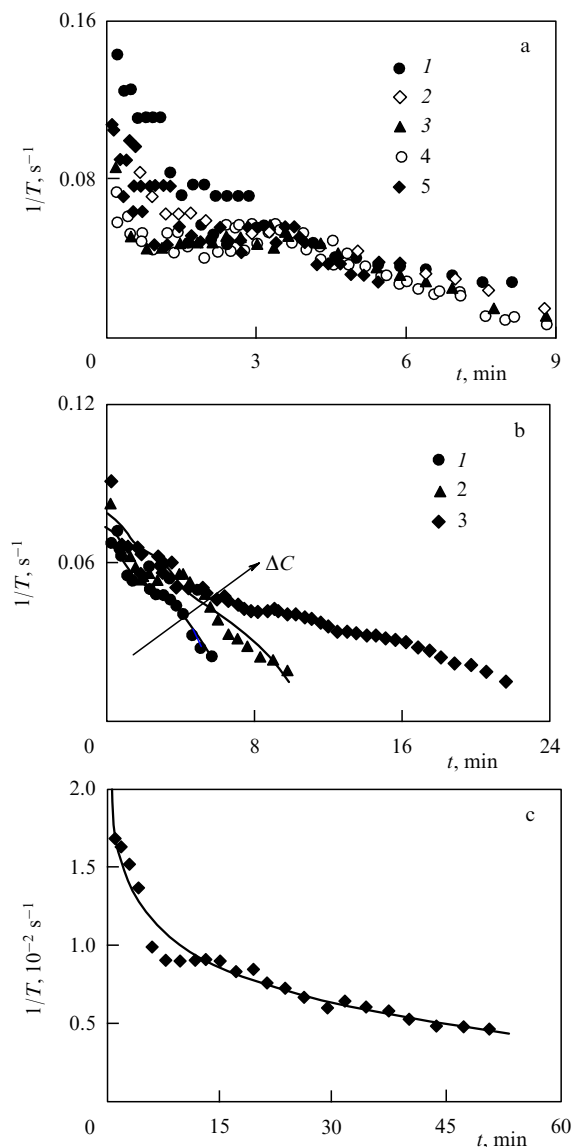


Figure 3. Time dependences of the frequency of oscillations in a two-layer system of liquids: (a) water–acetic acid solution, concentration difference $\Delta C = 70\%$, bubble diameter $d = 15.0$ (1), 10.7 (2), 7.1 (3), 5.1 (4), and 2.4 (5) mm; (b) water–acetic acid solution, $\Delta C = 20$ (1), 40 (2), and 70 (3)%, $d = 4.8-5.9$ mm; (c) 40 and 70% acetic acid solutions, $d = 5.1$ mm.

dependences show that, with an increase in the bubble diameter, the oscillation frequency only slightly decreased. In addition, oscillations halted faster in the case of bubbles of small diameters. The use of an additional set of cells showed that, at a constant initial concentration drop, the oscillation period increased with increasing layer thickness. A similar increase in the period was also observed with a decrease in the initial difference in concentrations (Fig. 3b). Characteristic of all the selected surfactants is the fact that the oscillatory mode stops completely unexpectedly at a finite value of the period, while a vertical concentration gradient still persists in the layer. Looking ahead, we point out that the reason for such a sudden halt of oscillations along with the absence of Marangoni convection at small initial concentration differences is the presence of uncontrolled surface-active impurities, which are due to an insufficient degree of purification of both water and the surfactants themselves.

In concluding this section, it should be noted that the period and duration of oscillations are definitely determined not by the surfactant concentration difference *per se* but by the corresponding difference in the values of surface tension $\Delta\sigma$, since the dependence of σ on concentration is nonlinear. Figure 3c shows the time dependence of the oscillation frequency for a two-layer system consisting of 40% and 70% acetic acid solutions ($\Delta\sigma \sim 5 \text{ dyn cm}^{-1}$). This system features a significantly smaller difference in surface tension compared with the ‘water–30% acetic acid solution’ system ($\Delta\sigma \sim 31 \text{ dyn cm}^{-1}$), and, consequently, with the same initial difference in concentrations, the intensity of the resulting Marangoni convection is lower. As a result, the oscillation period increases to several minutes, and the duration of the oscillation mode increases to several hours.

2.2 Bubble in a vertical layer of a stratified surfactant solution

Despite the obtained dependences of the period of oscillations on the concentration difference, characteristic dimensions of the layer, and diameter of bubbles, the experiment with a horizontal layer provides no information whatsoever about either the structure or the evolution of flows and distributions of the surfactant concentration near the bubble, or, most importantly, about the nature of interactions of capillary motion with other mechanisms of mass transfer during the formation of an oscillatory flow regime. Given that the most likely mechanism competing with the capillary one is gravity, observation should be carried out from a direction orthogonal to the gravity vector, which implies the use of a vertically oriented Hele-Shaw cell. To this end, a cell with gap $a = 1.2 \text{ mm}$ was installed on a narrow face, which was sequentially filled with distilled water and an aqueous solution of surfactant to create a stable two-layer system of liquids with a narrow diffusion mixing zone [75, 77, 78]. Aqueous solutions of isopropyl alcohol with $C_0 = 10-50\%$ and acetic acid with $C_0 = 30-70\%$ were chosen as surfactants. The selection of such ranges is due to the maximum difference in surface tension between the surfactant used and water [79] and the monotone dependences of the density, viscosity, surface tension, and refractive index of these solutions [80] (see Table).

The distribution of surfactants in the solution was visualized as a system of isolines of the refractive index, the value of which in the isothermal case depends on the concentration of the solution. The difference in the refractive index values of two adjacent monochromatic interference fringes calculated for a cell of a given thickness was 0.27×10^{-3} . Taking into account the nonlinear form of the concentration dependences of the refractive index, this corresponded to a change in the surfactant concentration in the solution of $0.40-0.75\%$ for acetic acid and $0.2-0.45\%$ for isopropyl alcohol (the difference between the concentrations of interference fringes decreases with an increase in the average concentration of the solution).

The gas bubble was placed into the cell using a medical syringe. Since the initial bubble diameter was larger than the layer thickness, the bubble took the form of a short wide horizontal cylinder with flat ends and a free lateral surface. A wire frame in the form of a flattened thin ring was used to prevent the bubble from rising under the effect of the Archimedes force. The frame, which left most of the lateral surface of the bubble free, did not hinder the development of Marangoni convection. The observations were made from the

Table. Properties of the solutions of the liquids used in experiments.

Methyl alcohol			
C, %	$\rho, 10^3 \text{ kg m}^{-3}$	$\eta, 10^{-3} \text{ kg (m s)}^{-1}$	$\sigma, 10^{-3} \text{ N m}^{-1}$
0	0.9982	1.002	72.0
10	0.9815	1.320	51.1
20	0.9666	1.580	40.5
30	0.9515	1.780	34.6
40	0.9345	1.840	31.0
50	0.9156	1.760	29.0
60	0.8946	1.600	27.6
70	0.8715	1.390	26.4
80	0.8469	1.140	25.2
90	0.8202	0.860	23.9
100	0.7917	0.580	22.2
Ethyl alcohol			
C, %	$\rho, 10^3 \text{ kg m}^{-3}$	$\eta, 10^{-3} \text{ kg (m s)}^{-1}$	$\sigma, 10^{-3} \text{ N m}^{-1}$
0	0.99823	1.002	72.0
10	0.98187	1.538	47.5
20	0.96864	2.183	38.0
30	0.95382	2.644	33.0
40	0.93518	2.910	30.2
50	0.91384	2.870	28.0
60	0.89113	2.670	26.2
70	0.86766	2.370	25.0
80	0.84344	2.008	23.8
90	0.81797	1.610	22.7
100	0.78934	1.200	21.8
Isopropyl alcohol			
C, %	$\rho, 10^3 \text{ kg m}^{-3}$	$\eta, 10^{-3} \text{ kg (m s)}^{-1}$	$\sigma, 10^{-3} \text{ N m}^{-1}$
0	0.9982	1.002	72.0
10	0.9821	1.740	40.4
20	0.9703	2.341	30.6
30	0.9520	2.835	26.8
40	0.9310	3.188	25.3
50	0.9069	3.383	24.3
60	0.8825	3.413	23.5
70	0.8584	3.293	22.7
80	0.8342	3.048	22.1
90	0.8096	2.724	21.7
100	0.7854	2.377	21.2
Acetic acid			
C, %	$\rho, 10^3 \text{ kg m}^{-3}$	$\eta, 10^{-3} \text{ kg (m s)}^{-1}$	$\sigma, 10^{-3} \text{ N m}^{-1}$
0	0.9982	1.002	72.0
10	1.0125	1.220	51.4
20	1.0263	1.450	43.3
30	1.0384	1.700	41.2
40	1.0488	1.960	38.2
50	1.0575	2.210	37.4
60	1.0642	2.430	36.1
70	1.0685	2.660	33.5
80	1.0700	2.750	31.5
90	1.0661	2.430	30.2
100	1.0498	1.220	27.8

side of the wide faces of the Hele-Shaw cell. Due to the small thickness of the cell, the emerging flows and concentration distributions can be considered two-dimensional. The bubble was usually placed in the diffusion mixing zone at the interface with the initial solution layer (as a reference area for subsequent calculation of the concentration distribution). The introduction of a bubble into a stratified surfactant solution set in motion tangential capillary forces on the lateral surface of the bubble, which caused the development of Marangoni convection.

Figure 4 shows a typical interference pattern of the concentration field around the bubble in a system of liquids which consisted of water on the top and a 70% solution of acetic acid on the bottom (the downward gradient of surfactant concentration and, correspondingly, the upward gradient of σ , which caused the motion of the surface to the upper pole of the bubble.) The height of the bubble slightly deformed by the gravity force was 3.8 mm, and its width was 6.0 mm. It is clearly seen that, first, the emerged capillary motion entrained the solution saturated with surfactant from the lower pole region upward, forming a thin layer around the bubble (Fig. 4a). Due to large characteristic times of diffusion, the transported surfactant did not have time to fully dissolve in the surrounding liquid and accumulated near the upper pole as a kind of denser ‘cap’. However, the layer with the uniform concentration that formed around the bubble significantly decreased the difference between pole concentrations, which is the source of Marangoni connection. As soon as the upward capillary motion reduced intensity, the dynamic equilibrium of the ‘cap’ was violated. Under the effect of the Archimedes force, the acetic acid flows first started moving downward to the right and left of the bubble (Fig. 4b). Due to the continuity of liquid, this motion was, in turn, accompanied by the formation under the bubble of a flow directed upward, which carried the solution with the higher surfactant concentration to the lower pole of the bubble (Fig. 4c).

The restoration of the difference between surfactant concentrations near bubble poles again reactivated the Marangoni forces, which strongly enhanced the upward flow. As a result, near the lateral surface of the cylindrical bubble, an intense convection motion emerged in the form of two symmetric vortices. In the process of evolution, these vortices captured an increasingly large volume of the solution with a high surfactant concentration. As a result, the average density of the solution in the interior of the vortices increased; they gradually moved downward (Fig. 4d) and, at a certain moment, blocked the supply of the surfactant to the lower pole of the bubble (Fig. 4e). As soon as this occurred, the intense convective motion rapidly halted. The duration of the entire process of the development and decay of this motion was no more than 30 s. Furthermore, under the effect of the gravity force, an advective motion developed in the cavity, which gradually restored vertical stratification by density (and concentration). As soon as the concentration difference along the lateral surface of the bubble attained the threshold value (Fig. 4f), the process iterated. These oscillations occurred with a period of about 1–2 min and could continue up to several hours until the external stratification of the surfactant concentration persisted. Gradually, the size of the region of the homogeneous solution below the bubble increased due to the mixing effect of the vortex cells, which resulted in an increase in the period and a decrease in the intensity of capillary convection.

In the experiments with isopropyl alcohol, where the surface tension gradient was oriented in the opposite direction (water was at the bottom), the emerging structure of the field of concentrations and flows was mirror-symmetric with respect to the horizontal diameter of the bubble. Alcohol was transported along the surface of the bubble to its lower pole, and periodically initiated convective vortices rotated in the opposite direction (in comparison with those in the experiments with a solution of acids.) A homogeneous zone was formed above the bubble.

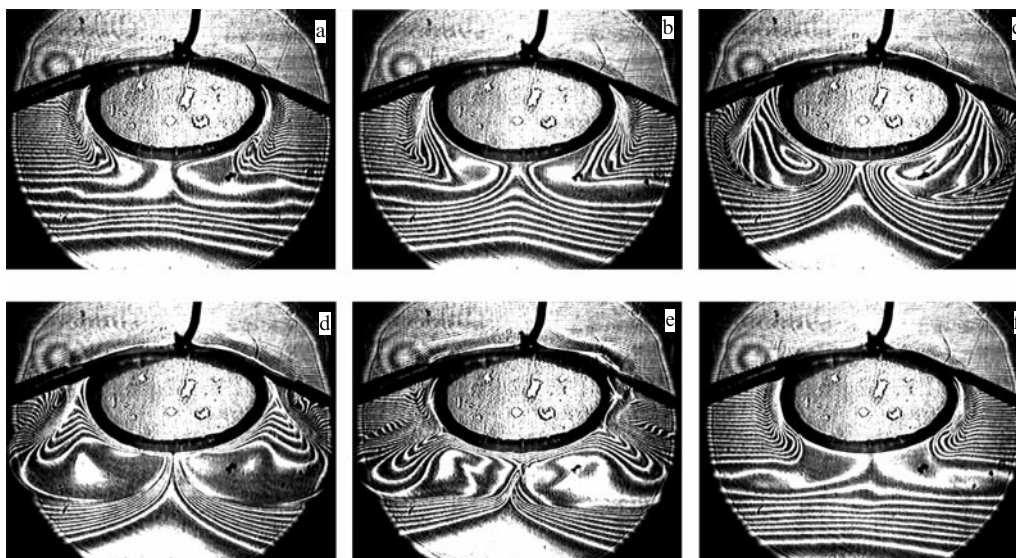


Figure 4. Evolution of the distribution of acetic acid concentration near an air bubble during first oscillation cycle: (a) $t = 0$, (b) $t = 2.25$ s, (c) $t = 4.5$ s, (d) $t = 8.25$ s, (e) $t = 12.0$ s, and (f) $t = 72.0$ s. Concentration difference between bubble poles $\Delta C = 10\%$. Side view.

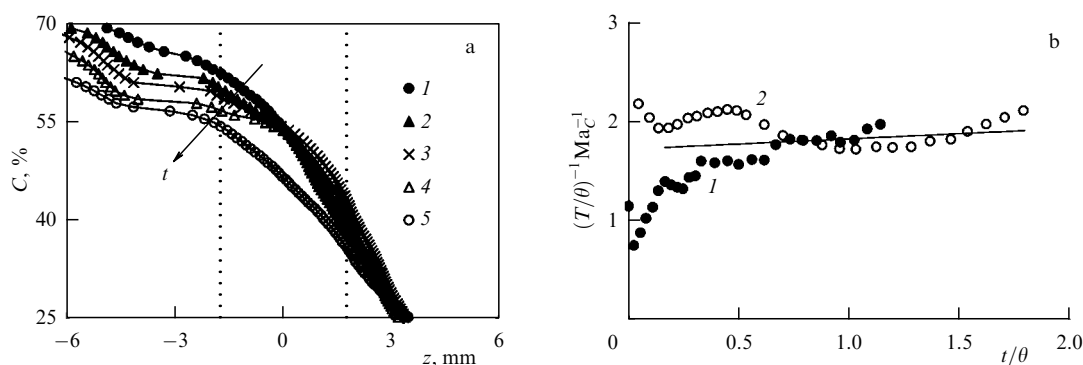


Figure 5. (a) Acetic acid concentration as a function of the vertical coordinate for a solution with $C_0 = 70\%$ at time points 0 (1), 15 (2), 30 (3), 60 (4), and 210 (5) min. (b) Time dependence of dimensionless vibration frequency, referring to the solutal Marangoni number: 1 — isopropyl alcohol, 2 — acetic acid. Straight line is plotted using the least squares method.

Figure 5a shows the distribution of the concentration of acetic acid along the vertical near the bubble in a solution with $C_0 = 70\%$ at different times. Dashed lines correspond to the lower and upper boundaries of the bubble. Measurements were carried out at the moments of time that precede the beginning of the selected cycles of oscillations, when the intensity of the convective motion was minimal. It is clearly seen that, in the ‘water-acetic acid solution’ system at the initial moment of time, the concentration decreased monotonically with increasing height (curve 1). Then, the bubble began to actively mix the surrounding liquid, reducing both the concentration difference between its poles (curves 2–5) and the concentration of the solution below it. At the initial moment, the vertical concentration gradient was maximum and amounted to 6.5% per mm. The corresponding values of the solutal Marangoni number $Ma_C = \sigma'_C \nabla C h^2 / (\eta D)$ and the Grashof number $Gr_C = \rho g \beta_C h^4 \nabla C / \eta^2$ (here, h is the bubble height) were 4.1×10^6 and 1.9×10^3 . Subsequently, the surfactant concentration gradient sharply decreased with time, approximately 60 minutes after the onset of oscillations, reaching a minimum value of 4.4% per mm ($Ma_C = 3.0 \times 10^6$, $Gr_C = 1.4 \times 10^3$), after which it again slowly increased to 5.2% per mm ($Ma_C = 3.1 \times 10^6$, $Gr_C = 2.0 \times 10^3$), to remain constant afterward. This re-

increase in the surfactant gradient is associated with an increase in the relative contributions of diffusion and large-scale gravitational flow to the concentration distribution around the bubble as the intensity of capillary motion decreases. A similar, albeit less pronounced, behavior of the concentration gradient was also observed in experiments with the ‘water–isopropyl alcohol’ system, which was probably due to the lower intensity of the convective motion due to the high viscosity of the solutions of this alcohol. In the experiments with alcohol solutions with $C_0 \leq 20\%$, the concentration gradient decreased monotonically.

The time dependence of the oscillation period was studied for various values of the average concentration of the solution, the concentration gradient, and the Marangoni and Grashof diffusion numbers. It has been established that the period of convective oscillations changes concurrently with the change in the concentration gradient. For example, in experiments with a 20% solution of isopropyl alcohol, the period increased monotonically with time to reach a maximum during the first hour, after which it remained unchanged. In experiments with a solution of acetic acid, the oscillation period also increased during the first hour, but then began to decrease, thereby indicating that the time dependence of the period was in inverse proportion to the

concentration gradient. Thus, in both cases, a proportionality was observed between the frequency (inverse period) of oscillations and the concentration gradient of the surrounding liquid. In Figure 5b, the dimensionless frequency normalized to the solutal Marangoni number is plotted on the ordinate axis, and the dimensionless time t/θ is plotted along the abscissa axis (viscous time $\theta = \rho h^2/\eta$ is chosen as the unit). The figure shows that, as soon as oscillations arise, the ratio $(T/\theta)^{-1} \text{Ma}_C^{-1}$ becomes virtually the same for different liquids and remains constant throughout the experiment, regardless of the orientation of the concentration gradient. The result obtained confirms the assumption that it is the solutocapillary forces that are the main initiator of the periodic convective motion around the bubble in an inhomogeneous liquid surfactant solution.

2.3 Mass transfer between a drop and an inhomogeneous surfactant solution (vertical layer)

Replacing a gas bubble with a drop of insoluble liquid significantly complicates the problem. First, due to the presence of the second contacting liquid phase, the surfactant can not only be adsorbed on the interface, but also can penetrate into the depth of the drop. The direction of surfactant diffusion is generally determined by the ratio of chemical potentials, the magnitude of which depends on the local concentration. A situation is possible in which, in an inhomogeneous solution, a surfactant absorbed in one part of the drop and then transferred by the flow to another area of the same drop exceeds there the limiting concentration that corresponds to the equality of chemical potentials at the interface and is forced to diffuse from the drop back into solution. Second, the capillary motion of the interface entrains the adjacent layers on both sides of the droplet surface. The emerging flow is able to span the entire volume of the drop due to its smallness. If the absorbed surfactant density is different from that of the base liquid of the drop, a gravitational flow occurs in the drop in addition to the capillary flow. Depending on the ratios of densities and the direction of the surface tension gradient, the capillary mechanism of motion either enhances the effect of the gravitational one or begins to compete with it. It should be noted that, if the surfactant concentration gradient is uniform in the solution, the intensity of capillary convection decreases in proportion to the drop diameter squared, while the gravitational motion weakens in proportion to the fourth power of the drop size.

Third, contacting insoluble liquids in many cases are good solvents for a significant part of uncontrolled surface-active impurities. As a result, the composition and concentration of surfactants at the interface may turn out to be less diverse and lower than at the free boundary. Consequently, the threshold for the development of Marangoni convection decreases, and the duration of the oscillatory regime increases. Fourth, the diffusion of a common solvent in a system of two immiscible liquids is often accompanied by the formation of an emulsion of one liquid in another, which was theoretically predicted in [81]. Due to the phenomenon of total reflection of light, transparent emulsion microdroplets look white in reflected light and dark in transmitted light; therefore, they can be used in experiments as light-scattering particles. Fifth, the dynamics of flows in the droplet-environment system are determined by the physicochemical properties of both media. In particular, this leads to a greater inertia of motion after the decay of an intense capillary flow, which can cause a change in the oscillation frequency.

In this experiment, to obtain quantitative data, a cylindrical drop is used, which is held in a stationary state by the gap walls. Some restrictions on the extension of the obtained results to the case of spherical drops should be noted. For example, the similarity of flows and concentration fields in spherical and cylindrical drops can only be assumed if the gap containing the drop is vertically oriented. In this case, the use of data on the behavior of a cylindrical drop is reduced to the case where two main flows arise in a spherical drop: toroidal (symmetric with respect to the vertical axis of the drop) or two-vortex (symmetric with respect to the vertical plane) [82]. It is also necessary to take into account the fact that the presence of solid boundaries, the role of which is played by the flat ends of a cylindrical drop, significantly reduces the flow velocity and reduces the surface area of the drop involved in mass transfer; consequently, the characteristic times of the studied stages of surfactant absorption change.

Taking into account these factors, an experiment was carried out to study the mass transfer between a drop of chlorobenzene and a stratified aqueous solution of isopropyl alcohol, which filled a vertical Hele-Shaw cell [83]. It should be noted that isopropanol is lighter than water and chlorobenzene ($\rho = 1.1066 \text{ g cm}^{-3}$), exhibits surface-active properties in relation to both liquids and is highly soluble in them, while the maximum solubility of pure chlorobenzene in water is only 0.05% (at $T = 30^\circ\text{C}$), and the solubility of water in chlorobenzene is even lower. These data enable making an assumption that, at low initial concentrations of alcohol, a drop only absorbs alcohol from the surrounding solution, and the counter flow of chlorobenzene is negligible (counter flows should be taken into account if the concentration of alcohol in water exceeds 30% [84]).

For the experiment, a vertical Hele-Shaw cell, previously used in experiments with a gas bubble, was equipped with an additional liquid container at the top and a drain tube at the bottom. A Fizeau interferometer was used to visualize the surfactant distribution from the side of the wide faces of the cell as a system of equal concentration lines. The transition from one fringe to another corresponded to a change in the concentration of isopropyl alcohol by 0.22–0.27% in water (depending on its average concentration) and by 0.10% in chlorobenzene. Before the start of the experiment, the cell was filled with distilled water, and an additional container was filled with a solution of isopropyl alcohol with a given concentration ($C_0 \leq 20\%$). Next, a drop of chlorobenzene was introduced into the cell using a syringe. Having touched the walls of the cell, it took the form of a wide short cylinder with diameter D_0 ranging from 2 to 15 mm. After that, the water was drained, and the isopropanol solution concurrently spread downward. The water drain stopped when the drop was in the zone of diffusion transition between the layers of water and alcohol. The experiments were carried out at an ambient temperature of $(21 \pm 1)^\circ\text{C}$.

As expected, the creation of a surfactant concentration gradient along the lateral surface of the drop led to the onset of an oscillatory mass transfer regime. Figure 6 shows a series of interferograms that describe the evolution of the alcohol concentration distribution during one oscillation cycle (corresponding numbers $\text{Ma}_C = 6.3 \times 10^7$, $\text{Gr}_C = 1.7 \times 10^4$). The first interferogram (Fig. 6a) was obtained immediately before the start of the cycle. By that moment, a characteristic distribution of absorbed alcohol had already formed inside the drop, with a small difference in concentration in the main volume of the drop and a large difference near

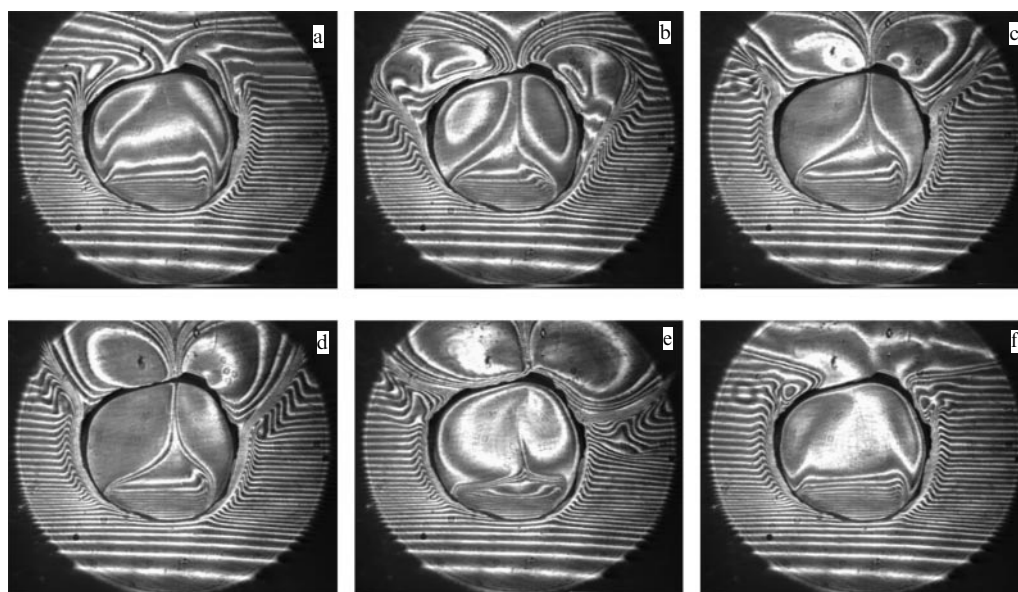


Figure 6. Evolution of the concentration field of isopropyl alcohol during its diffusion into a drop from a stratified solution. Time from the beginning of the capillary movement intensification cycle: (a) $t = 1$ s, (b) $t = 5$ s, (c) $t = 16$ s, (d) $t = 24$ s, (e) $t = 45$ s, (f) $t = 68$ s.

its lower pole. The distribution emerges due to gravity: since alcohol is lighter than chlorobenzene, its diffusion into the drop causes an intense convective flow that mixes the solution, while chlorobenzene with a low alcohol content accumulates at the bottom, forming a stagnant zone. In the presence of such a difference in surfactant concentration inside the drop along its lateral interfacial surface, a nonzero surfactant concentration gradient persists, and, consequently, a weak capillary flow is maintained. Over time, this flow is enhanced, since the advective (gravitational) flow, as in the case of a bubble, restores the initial concentration stratification, including the vicinity of the lower pole of the drop. A decrease in the concentration in the exterior results in the diffusion of the surfactant from the drop, causing a decrease in its concentration already inside the drop: as a result, the concentration difference between the lower and upper poles of the drop increases. The intensity of the capillary flow gradually increases, and it entrains increasingly large volumes of solution into motion.

A ‘burst’ of capillary motion occurs when the surface of the drop is reached by the flow of a solution with an increased concentration of alcohol from the area above the drop, which is the beginning of a new cycle (Fig. 6b). This flow, partially transferring alcohol to the drop, moves downward along the interface until the increasing Archimedes force compensates for the action of capillary forces. Then, the solution floats up, forming convective cells on both sides of the drop. It should be noted that the reversal zone of the downward motion is clearly visible in the interferogram as the region of closure of the envelope of the drop stagnation zone and the interface. Similar symmetrical cells, separated by a convective torch, are also formed inside the drop. External convective cells created by an alcohol solution that is lighter than the environment quickly shift to the upper pole of the drop (Fig. 6c). Their further ascent is hindered by jets of a solution flowing to the drop with an even higher concentration of alcohol. With further intensification of the capillary flow, the cells continue to be replenished with the solution, increasing in size (mainly along the vertical) (Fig. 6d). They gradually

move up and, finally, closing up, cut off the supporting flow of alcohol from the drop (Fig. 6e). As a result, the capillary movement stops almost instantly, followed by the cellular flow. The convective cells above the drop are destroyed, and the alcohol solution spreads along the equal density plane, giving rise to advective motion. Such a movement, which can engage the surrounding solution at a distance of several diameters of the drop to the right and left of it, restores the vertical stratification of the surfactant solution. The vertical distribution of the concentration is also restored inside the drop, and a chlorobenzene solution with a significant alcohol concentration floats up, which until now has been retained by capillary motion in the lower part of the drop and along its side surface (Fig. 6f). Since after several cycles the average concentration of alcohol in the drop has already reached the equilibrium value, the solution floating up has an excess concentration, and the drop needs to reduce it by diffusion of alcohol into the environment. All these processes result in a slow recovery of the surfactant concentration drop along the interface and the development of capillary motion. Then the cycle repeats.

The processing of interferograms obtained in real time made it possible to trace the change in the alcohol concentration at selected points inside and outside the drop both during the cycle and throughout the oscillatory regime. It was found that the presence of a second liquid phase with its own viscosity and density significantly complicates the time dependence of the flow oscillation period (Fig. 7a). A certain similarity with intermittency in turbulence is clearly traced, since three types of flows concurrently interact with different characteristic times, determined by the dimensions of the cavity and inclusion and different mechanisms of motion. These currents are: (a) a large-scale advective flow of a solution in the environment that supports density stratification; (b) a capillary flow along the surface of the drop, leading to local destruction of this stratification; (c) a free convective motion in the drop, the intensity of which is determined by the balance of gravity, capillarity, and diffusion. As a result, a long period is preceded by several ‘false starts’, when the

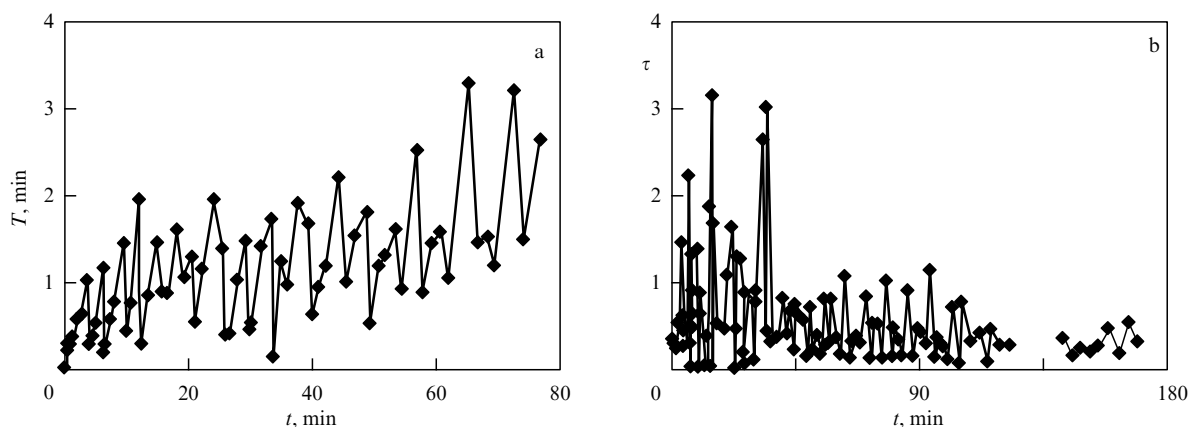


Figure 7. (a) Time dependence of the oscillatory regime period. Initial concentration of an aqueous solution of isopropyl alcohol is $C_0 = 20\%$, drop diameter is $D_0 = 6.0$ mm. (b) Relationship between times of dominance of capillary and gravitational convection.

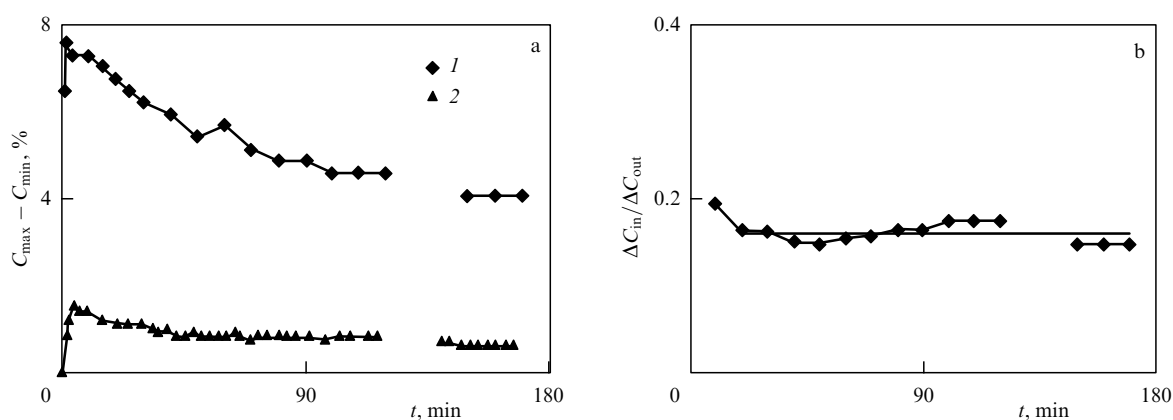


Figure 8. (a) Time dependence of the difference between alcohol concentrations inside and outside the drop (curves 2 and 1) between its poles. (b) Change in the ratio of the difference between concentrations inside and near the drop with time from the beginning of the development of the oscillatory regime.

emerging capillary movement quickly decays, since it is not supported by the flow of a sufficient amount of fresh solution. However, the ‘false start’ intensifies the advective flow, which, after a few ‘shocks’, gains the velocity necessary for the development of a sustained capillary movement. This conclusion is suggested by an analysis of the ratio $\tau \equiv t_c/t_g$ of two times, which in total make up the period itself: the times of the predominance of capillary and gravitational convection within one cycle (Fig. 7b). It is clearly seen that each period with prolonged capillary motion ($\tau > 1$) is preceded by several periods during which gravitational convection prevails ($\tau < 1$).

Figure 8a shows the time dependence of the difference in alcohol concentrations inside and outside the drop (curves 2 and 1, respectively) between its poles. It can be seen that, despite the complex form of the concentration field and the high degree of its nonstationarity, the drop responds to changes in the external concentration with virtually no time delay due to the high intensity of Marangoni convection. It should be noted that the interruption of curves 1 and 2 at a time value of about 120 min is associated with the video recording of the flow structure at this time using light-scattering particles. Figure 8b shows the dependence of the ratio of the concentration difference inside and near the drop on the time from the moment when the development of the oscillatory regime starts. As can be seen, the approximation curve is virtually independent of time, with the

exception of the initial stage (8–10 min) of the onset of the current oscillation mode, and the obtained value agrees with good accuracy with the corresponding value for the equilibrium distribution of isopropyl alcohol in the chlorobenzene–water system for a given concentration of alcohol in water [84].

Another feature characteristic of drops in a stratified solution should be noted. To maintain the oscillatory regime of mass transfer, it is sufficient to maintain the value of the alcohol gradient $\nabla C \sim 1\%$ per cm, while, in the case of gas bubbles, the corresponding value is much larger. Therefore, the duration of oscillatory regimes for drops can significantly exceed that for gas bubbles for the same surfactant concentration gradients and can be as large as several ten hours. This phenomenon is a consequence of a decrease in the concentration of uncontrolled surface-active impurities at the interface compared to the concentration on the free surface. It should be recalled as well that the characteristic times of saturation of a drop with a surfactant from its homogeneous solution are only about 15–20 min for drops with a diameter of about 6 mm, most of the conditions being the same (a vertical layer, the presence of capillary and free convection, and the same value of average surfactant concentrations).

It is noteworthy that the development of such oscillatory regimes near bubbles and drops in stratified surfactant solutions was observed somewhat later by other groups of researchers [85].

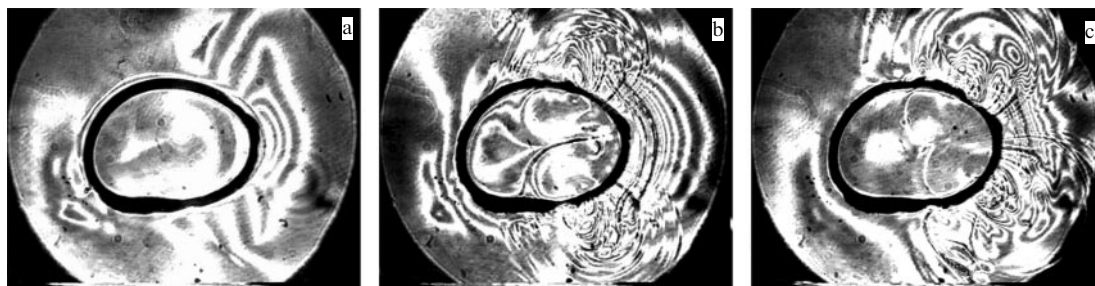


Figure 9. Absorption of alcohol by a drop from an inhomogeneous solution at $\Delta C = 30\%$, $D_0 = 6.0$ mm. (a) $t = 2$ s, (b) $t = 7$ s, and (c) $t = 25$ s.

2.4 Mass transfer between a drop and an inhomogeneous surfactant solution (horizontal layer)

The creation of a cylindrical drop in a thin horizontal layer with a vertical gradient of surfactant concentration not only reduces its vertical size, consequently changing the ratio of intensities of capillary and gravitational convection, but also significantly alters the conditions for mass transfer between the drop and the environment [83]. In a horizontal layer, the area of surfactant absorption and the development of accompanying motion is reduced for a drop to the size of the layer. As a result, in the case of the development of Marangoni convection, similar to the flow in a vertical layer, it should quickly halt, since the formation of a small-sized convective cell is sufficient to cut off the ‘feeding’ surfactant flow from the drop. On the other hand, the time before the resumption of intensive movement is reduced, since, in this case, it is determined by the time of restoration of the vertical stratification of the solution under the effect of gravity. As a result, the period of the oscillatory regime of mass transfer can be somewhat reduced, as is observed in the case of a gas bubble in a horizontal channel with vertical stratification of the solution. However, an alternative version of the development of mass transfer in a horizontal layer is also possible. An increase in the length of the interfacial boundary of a drop in the horizontal direction increases the probability of the occurrence of a local inhomogeneity of surfactant absorption, which leads to the emergence of surfactant gradients along the drop surface. As a consequence, the capillary flow acquires a longitudinal component, which in turn leads to the formation of a complex advective flow near the drop. The movement with a vertical axis of symmetry is replaced by a three-dimensional flow, symmetrical with respect to the horizontal axis of the drop. It should be noted that, in this situation, due to such a flow structure, it is not possible to calculate the concentration distribution in the cavity; however, due to the large diffusion times and low viscosity, the changes in the position of the concentration isolines nevertheless enable determination of the flow structure and tracing its evolution.

Figure 9 shows a series of interferograms of the concentration field that occurs near a drop of chlorobenzene introduced into a horizontal layer 2.4 mm thick with a vertical difference in the concentration of isopropyl alcohol $\Delta C = 30\%$ (the corresponding values of the Marangoni diffusion number and the Grashof number are 6.5×10^6 and 4.5×10^2). At the beginning of the experiment, a solution with a higher surfactant concentration flows to the droplet along the upper boundary of the layer. Part of the surfactant from this flow diffuses into the droplet, while the remaining solution with a reduced surfactant concentration flows

down the interface (interference fringes are parallel to the droplet surface) (Fig. 9a). Then, the solution spreads along the cell bottom primarily on the right (this process is reflected in a system of concentric fringes centered on the drop surface). Local outflow triggers in the same part of the drop a prevailing inflow of alcohol with a high concentration (due to the continuity of the liquid). A difference in surfactant concentration occurs along the drop surface, and, as a result, the capillary flow forms external and internal convective cells that resemble the structure of the surfactant concentration field in a drop in a vertical layer (Fig. 9b). However, now the effect of gravity is orthogonal to the plane of the main capillary motion. An analysis of the interferogram in Fig. 9b shows that the capillary motion develops in the upper part of the layer, while the gravitational flow persists in the lower part of the layer. An increase in capillary cells over time leads to the overlapping of the areas of these flows and, as a result, the cellular flow breaks up into several parts (Fig. 9c) with the destruction of the feeding flow. When this happens, the motion in the layer plane halts, and the restoration of the vertical concentration stratification to the right of the drop begins. It should be noted that, at this moment, the left part of the drop and the solution adjacent to it are hardly involved in large-scale motion and retain vertical stratification. While the surfactant vertical gradient is being restored to the right of the drop, the mass transfer to the left of it loses stability, and the development of intense capillary motion is repeated this time on the left side of the drop.

Figure 10 shows the change in the frequency of flow oscillations as a function of time from the beginning of the

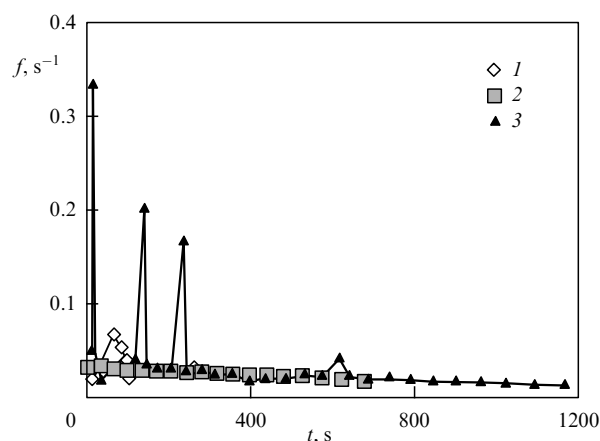


Figure 10. Change in the frequency of oscillations of the intensity of the mass transfer process over time for drops with various initial differences in isopropyl alcohol concentration: $\Delta C_0 = 7\%$ (1), $\Delta C_0 = 10\%$ (2), and $\Delta C_0 = 30\%$ (3).

oscillatory mass transfer regime for various values of the initial difference in the surfactant concentration in the horizontal layer. It is clearly seen that, in this situation, the oscillatory regime, in contrast to that in the case of a drop in a vertical layer with a vertical surfactant concentration gradient, features a relatively short duration, which increases with an increase in the initial difference in concentrations ΔC . In this case, the oscillation frequency, with the exception of the initial time interval, is virtually the same for different ΔC values. In addition, experiments with drops of various sizes (2–8 mm) have shown that the frequency slightly depends on the drop diameter. These observations suggest a conclusion that gravity has a significant effect, despite its apparent noninvolvement in the formation of large-scale motion.

3. Oscillatory regimes of concentration convection in a horizontal channel

3.1 Threshold development of Marangoni convection near bubbles and drops with a vertical interface

The experiments presented in Section 2, despite their clarity, feature one drawback: they are too complicated for numerical simulation and, consequently, the results obtained can only be used to interpret and predict phenomena in a fairly narrow range of physicochemical parameters. To create a database for theoretical and numerical studies, an experiment is needed with a different cavity and bubble/drop geometry while retaining the advantages of the Hele-Shaw cell (in particular, the two-dimensionality of flows). Such requirements for a cell are fulfilled by a narrow horizontal channel of a rectangular cross section, partitioned off by a vertical free or interphase boundary [75, 86–89]. Its geometry and boundary conditions make it possible to apply mesh methods for numerical simulation of flows and concentration fields.

To create such a channel in the experiment, a pair of solid inserts were installed in a vertical Hele-Shaw cell, which formed a horizontal channel with length $l = 20$ mm, height $h = 2$ mm, and width $b = 1.2$ mm (Fig. 1b). The channel at one end adjoined the side wall of the cell with a glued hollow needle for making a bubble. The opposite end of the channel remained open. A two-layer system was created in the cell: a ‘distilled water–surfactant’ aqueous solution with a given thickness of the transition (diffusion) zone between them. Methyl, ethyl, or isopropyl alcohols of ‘chemically pure’ degree of purification were used as surfactants. By changing the water level (as the lower layer), the channel could be pre-filled with a stratified solution, or such a stratification could be formed already in the course of the experiment. In the former case, the bubble introduced into the channel was immediately located in the surfactant gradient solution; in the latter case, the solution flowed to the bubble pre-installed in the water in the form of a ‘tongue’ along the upper boundary of the channel.

In both cases, the emergence of a surfactant concentration difference along the surface of the bubble led to the development of Marangoni convection and the onset of an oscillatory regime (as in the case of a bubble in an inhomogeneous surfactant solution in a vertical layer). A similar result was obtained by Birikh and Rudakov in a numerical study based on a model of convection with diffusive transport of surfactants to the bubble surface (without the formation of a surface phase) in [86]. In this study, a horizontally elongated rectangular cavity was

considered, one of the vertical boundaries of which modeled the bubble surface impermeable to surfactants. At the second lateral boundary, the initial vertical gradient of surfactant concentration was set, which subsequently generated a longitudinal gradient (an analog of the inflowing ‘tongue’). Calculations have shown that, at large values of the Schmidt number ($\sim 10^3$), self-oscillating modes of concentration flows developed in the cavity. Against the background of slow gravitational convection, short bursts an order of magnitude more intense than Marangoni convection were observed. The results of the experiment and numerical calculation are in good agreement in what regards the structure of the convective motion and the oscillation period.

A result of the experiment was the discovery of the phenomenon of delay in the development of the Marangoni flow relative to the moment when the free surface of the bubble is touched by an inhomogeneous surfactant flow. To investigate the mechanisms of such a delay, the following series of experiments was carried out. Figure 11 shows two series of interferograms of the concentration field evolution near the side boundaries of an air bubble and a chlorobenzene drop when the ‘tongue’ of an isopropyl alcohol solution is inflowing in a horizontal channel. It is shown that the solutocapillary flow does not develop immediately after the surfactant ‘tongue’ reaches the bubble surface, but only after some time has elapsed. For example, in the experiment with an air bubble (Fig. 11a, b), the time interval Δt between the moment the surfactant touched the surface and the moment the convective vortex appeared (Fig. 11c) was 28 s, while the concentration difference ΔC^* in the lower and upper poles of the bubble reached 2.2%. Then, the equilibrium was suddenly disturbed and very rapidly (within about 0.2 s) an intense Marangoni flow burst out in the form of a vortex cell, in which the surfactant, entrained by capillary forces, was transported along the surface of the bubble to its lower pole (Fig. 11d). Due to the continuity of the liquid, the emerging flow accelerated the inflow of a concentrated surfactant

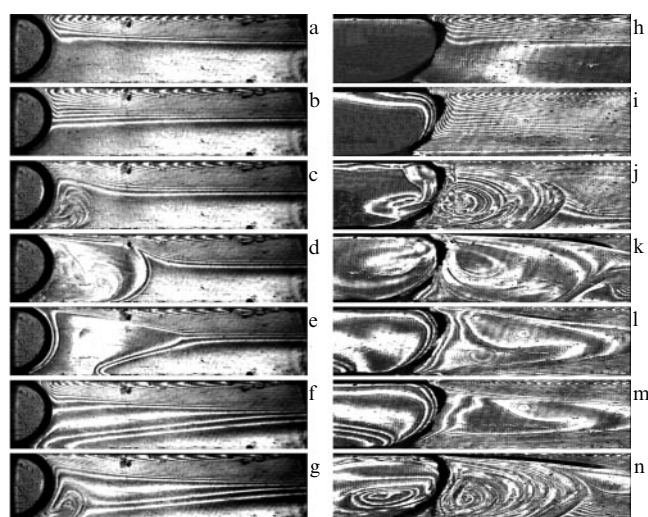


Figure 11. Evolution of the concentration field near a vertical interface in an inhomogeneous solution of isopropyl alcohol in a horizontal channel. Air bubble, time from touching the surfactant ‘tongue’: (a) $t = 0$, (b) $t = 28.0$ s, (c) $t = 28.1$ s, (d) $t = 28.2$ s, (e) $t = 29.2$ s, (f) $t = 34.2$ s, (g) $t = 34.3$ s. A drop of chlorobenzene, time from the moment of touching the surfactant ‘tongue’: (h) $t = 0$, (i) $t = 60$ s, (j) $t = 61$ s, (k) $t = 66$ s, (l) $t = 70$ s, (m) $t = 76$ s, (n) $t = 77$ s.

solution to the bubble surface along the upper boundary of the cavity, thereby intensifying the convective vortex even more. However, while developing and capturing an increasing amount of a solution with a high surfactant concentration, the vortex cell became lighter and, rising up, cut off the incoming flow of alcohol. As a result, the vortex flow stopped abruptly, and the bubble surface turned out to be surrounded by a thin layer of liquid with the same surfactant concentration (Fig. 11e). The decay of the capillary flow by no means meant that the motion of the liquid in the channel stopped, since the advective flow again pulled a more concentrated surfactant solution to the upper pole of the bubble. After the surfactant flow touched the surface, a capillary vortex arose again (Fig. 11f, g). The cycle was repeated many times, the period of oscillations increased with time, and the intensity of the vortex flow decreased, which was due to a gradual decrease in the vertical concentration gradient in the solution due to convective mixing. The Marangoni convection stopped when the concentration in the channel was almost completely leveled.

A similar pattern was also observed at the interface of chlorobenzene drops in an isopropanol solution (Fig. 11h–n). Interferograms clearly show that alcohol reaches the surface of the drop and has time—before the development of convective motion begins—to diffuse through it, penetrating into chlorobenzene and creating a surfactant gradient in it. Initially, this process occurs fairly uniformly along the surface of the drop and, thus, there is no surfactant gradient on the surface itself. It is only later that intense Marangoni convection develops in the solution (at $\Delta t \sim 1$ min after the moment the surfactant ‘tongue’ touches the surface of the drop and at $\Delta C^* \sim 4\%$). It is characteristic that in the case of both a bubble and a drop, during all subsequent cycles after the first cycle, the development of capillary motion started already at much lower concentration differences along the surface (for example, for a bubble, the development of the second cycle occurred at $\Delta C^* \sim 0.6\%$ (Fig. 11f)). To determine the reasons for the decrease in the critical drop in the concentration ΔC^* and the corresponding critical value of the diffusion Marangoni number Ma_C^* , their dependence on the number of cycles from the moment the oscillatory regime is established was compared with a similar dependence of the average alcohol concentration C_{av} formed by the surrounding solution on the surface of the inclusion. Figure 12a shows the

dependence of the average concentration of two kinds of alcohol on the surface of the bubble at the beginning of the cycles. A comparison of the behavior of this dependence with the dynamics of the critical Marangoni number suggests a conclusion that the value of Ma_C^* decreases at approximately the same rate as C_{av} increases. It is primarily the surface tension which depends on the average surfactant concentration; it decreases with increasing surfactant content in the surrounding solution. In addition, with a decrease in the surface tension difference between the surfactant solution, which creates an inflowing ‘tongue’, and the liquid, which forms the free boundary of the bubble, the intensity of the capillary force effect decreases along with the probability of the occurrence of Marangoni convection at its threshold development (as can be concluded based on the presence of a threshold value of the Marangoni number in the experiment).

There may be another reason for the absence of surface movement: uncontrolled surface-active impurities [90, 91], the composition and concentration of which depend on the magnitude of surface tension, decreasing as σ decreases. In addition, with each subsequent cycle, the bubble is surrounded by a more concentrated solution. An increasing amount of alcohol comes to the surface of the bubble, as a result of which the adsorbed film of impurities changes its properties. This creates conditions for the development of capillary motion at a lower surface tension gradient.

Formally, it makes no difference in what way the surfactant concentration in the solution is set near the bubble surface. To verify this assumption, a series of experiments was carried out using homogeneous solutions of ethyl and isopropyl alcohols with C_0 ranging from 1 to 8% as the base liquid of the channel. The obtained data were used to plot the critical value of the Marangoni number that corresponds to the moment the first vortex emerges as a function of the initial content of surfactant in the solution surrounding the bubble. It was found that, as C_0 increases, the values of Ma_C^* decrease monotonically similarly to the case where the dependence of Ma_C^* on the concentration C_{av} at the beginning of each cycle was examined. A generalization of the results of the two series of experiments described above is shown in Fig. 12b as the dependence of the critical Marangoni number on the difference $\Delta\sigma$ of the surface tensions of water σ_0 and the solution near the interface ($\Delta\sigma = \sigma_0 - \sigma_C$). As can be seen, the

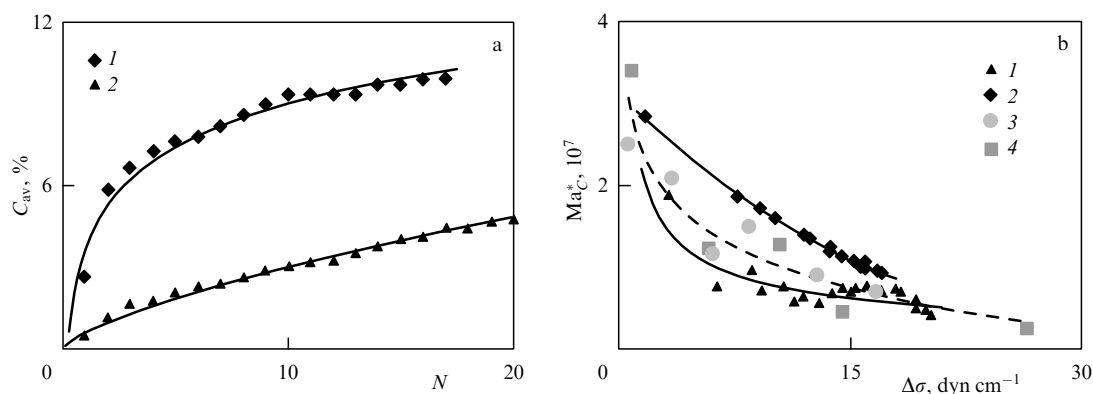


Figure 12. (a) Average surfactant concentration on a bubble surface at instants of capillary convection ‘bursts’ as a function of the number of cycles; 1 — ethyl alcohol, 2 — isopropyl alcohol. (b) Critical value of the Marangoni number as a function of the difference between surface tensions of water and solution at the onset of ‘bursts’ of capillary convection (1 — ethanol, 2 — isopropanol) and in the first cycle in surfactant solutions with various initial concentrations (3 — ethanol, 4 — isopropanol). Dashed line is the general curve.

Ma_C^* values obtained in various experiments and under various conditions turn out to be quite close in magnitude, and the shapes of all the curves agree well with each other. Thus, it actually does not matter in what way the surfactant concentration increases: either due to its influx and subsequent mixing of the solution during the intensification of capillary movement, or by initially achieving its high content in the base liquid. The capillary motion resumes on each cycle of the oscillatory mode when the critical Marangoni number, determined by the current state of the film of adsorbed impurities, is exceeded.

It is noteworthy that the change in time Δt of the delay in the development of Marangoni convection can also be explained by the effect of uncontrolled impurities. In the presence of impurities, the delay time is the sum of the diffusion time required for the controlled surfactant to reach the liquid surface and the time for the formation of its gradient along the liquid surface, which is necessary for the development of capillary motion. The first part is determined by Fick's first law (under the assumption of low surfactant concentrations, when the change in concentration with time in the selected cross section perpendicular to the direction of diffusion, which coincides in this case with the free surface, is proportional to the volume concentration gradient determined by the inflowing 'tongue'). The second part is related to the need for partial dissolution of the film of adsorbed impurities to a level sufficient for the formation of surface motion by shear stress created by the injected surfactant. In the case where the bubble is surrounded not by water, but by an alcohol solution, the mechanical properties of the film are initially reduced due to the presence of alcohol molecules in the surface layer. Consequently, Δt should decrease with increasing C_{av} , which is observed in the experiment.

Another implication of the effect of uncontrolled impurities is a sudden transition from the oscillatory mode of convection near the bubble/drop to a monotone flow, despite the fact that the difference in the surfactant concentrations in the cavity is still nonzero. It is clear that, at the time when the regime changes, the bubble (or drop) is surrounded by a surfactant solution, the average concentration of which determines the set of impurities. It can be assumed that the cessation of oscillations is associated with the attainment of a balance between the shear stress that occurs when a difference in surfactant concentrations appears and the stress created by the deformed impurity film already at the beginning of the cycle: the shear stress created by the surfactant decreases faster than the stress associated with the impurity film (diffusion times are much longer than the convective ones). The intensity of the capillary motion strongly decreases, although it does not vanish, since it is supported by a large-scale advective current.

Summing up, it should be noted that the oscillatory mode of mass transfer near the interface in inhomogeneous surfactant solutions is determined by the interaction between the capillary and gravitational mechanisms of fluid motion and, therefore, can occur in the absence of uncontrolled impurities. Nevertheless, surface-active impurities play an important role in the onset of this regime, setting the conditions for its development and switching and leveling its duration and period in each cycle. It should be pointed out that the determination of the degree of influence of uncontrolled impurities and the theoretical description of the processes at the interface with their participation, as well as the description of their interaction with temperature and

concentration gradients on the free surface, have been actively explored. For example, in a series of studies by Birikh [92–94] and in the study by Birikh, Pukhnachev, and Frolovskaya [95], assorted variants of the flow both in the case of a stationary impurity film and after its destruction were examined. Shmyrov and Mizev [96] experimentally studied the features of the development of a thermocapillary flow in the presence of an insoluble surfactant film with various surface concentrations.

3.2 Effect of surfactant surface activity on the period of oscillations

One of the main characteristics of a surfactant is its surface activity, i.e., the ability to lower surface tension during adsorption at the phase boundary. To determine it, the area of maximum change in surface tension at low concentrations of surfactant $G \equiv -\partial\sigma/\partial C|_{C \rightarrow 0}$ is used.

To assess the role of surface activity of surfactants in forming an oscillatory regime, we examine the evolution of the flow near an air bubble for solutions with low initial concentrations of several types of alcohol of the same homologous series. The choice of solutions with low C_0 is driven by the attempt to reduce the influence of the gravitational component of the advective flow. To reduce the error associated with the presence of surface-active impurities, triple deionized water, which was subject to preliminary distillation, was used to fill the channel and prepare surfactant solutions. Methyl HCH_2OH , isopropyl (propyl isomer) $H(CH_2)_3OH$, and amyl $H(CH_2)_5OH$ alcohols were selected for the experiment. The homologues were selected to enable application of the Duclos–Traube rule, according to which the surface activity of a homologue increases by a factor of 3–3.5 with an increase in the number of methylene groups ($-CH_2-$) by one [97, 98]. As a consequence, with an increase in the length of the alcohol molecule, an increase in its surface activity enables the attainment of threshold values of shear stresses at ever lower initial concentrations of solutions. In particular, in our series of experiments, ΔC^* for methyl, isopropyl, and amyl alcohols was 6.65, 3.5, and 0.25%, respectively. A decrease in the threshold concentration leads to a decrease in the density difference between water and a surfactant solution and, consequently, to a decrease in the effect of the Archimedes force. The latter, in turn, causes a change in the shape of the concentration 'tongue' with a concurrent decrease in the rate of its propagation in the channel. For example, at a threshold concentration of amyl alcohol (the corresponding density difference is $\Delta\rho \sim 0.003 \text{ g cm}^{-3}$), the concentration tongue occupies almost the entire channel cross section. As a result, it touches the surface of the bubble in the center of the channel, which leads to the emergence of two symmetrical convective cells instead of one. The intensification of the motion, however, leads to the predominant development of the lower cell, and, in subsequent cycles, the resulting motion already has a single-vortex form.

We also note that the bubble in the amyl alcohol solution had to be placed almost in front of the channel entrance from the side of the cell to achieve flow oscillation periods comparable to those for alcohols with a shorter molecule length. Otherwise, the low speed of propagation of the 'tongue' in the channel led to an increase in the oscillation period of up to several minutes. Thus, the distance from the bubble to the channel edge becomes another parameter of the problem (similar to the distance from the surfactant drop to

the free surface in the problem of Marangoni convection from a localized source of surfactant in a liquid volume [73]). In a further study, we used solutions of alcohols with a C_0 value at which a concentration difference ΔC occurs on the surface of the bubble that minimally exceeds the threshold value of ΔC^* . In this case, the start of the oscillatory motion was characterized by modified concentration Grashof Gr_C and Marangoni Ma_C numbers, equal to, respectively, 146 and 8.40×10^6 for a methyl alcohol solution with $C_0 = 8\%$; for an isopropyl alcohol solution with $C_0 = 6\%$, these numbers were 47.9 and 1.15×10^7 ; and for an amyl alcohol solution, $C_0 = 0.3\%$, 206 and 2.06×10^7 . The modified Grashof and Marangoni numbers were defined as $Gr_C = \rho g \beta_C C_0 h^4 / (\eta^2 L)$ and $Ma_C = \sigma'_C \Delta C (bh)^{0.5} / (\eta D)$, where L is the distance from the bubble to the open edge of the channel. The Grashof number introduced in the problem differs from the standard definition by the normalization coefficient h/L , which is the ratio of the squares of the characteristic times of the convective cell float up and the inflow of the surfactant solution along the channel. In the Marangoni number, the characteristic size is calculated using the area of the free surface (it is more expedient to use such a definition of Ma_C for small-area interfaces in the presence of uncontrolled impurities [99]).

All the above conclusions are confirmed by analyzing the influence of surface activity on the oscillatory regime based on comparing the flow oscillations in solutions of methyl and amyl alcohols (Fig. 13). As before, the time of one cycle can be represented as the sum of the times of dominance of the capillary (1) and gravitational (2) components of the concentration flow near the bubble, shown in pairs as elements of the diagram in Fig. 13. A comparison of the obtained dependences, and similar data on the isopropyl alcohol solution, shows that the times of capillary convection in the first cycle for all alcohols are virtually the same, amounting to about 3–4 s, despite a significant difference in surface activity. The high degree of purification of water and the various alcohols leads to the persistence of a virtually unchanged duration of the Marangoni convection during subsequent cycles. To level the period of oscillations in solutions of methyl and amyl alcohols, the distance from the bubble boundary to the open end of the channel was reduced for the latter by a factor of 20. As the comparison shows, the periods after such an operation turn out to be comparable, although the ratio of the times of the predominance of capillary and gravitational movements differs significantly.

In addition, since the critical concentration difference for methyl alcohol is about 25 times greater than that for amyl alcohol, for the former, the average concentration of the solution near the bubble increases noticeably with each subsequent cycle. As a result, the surface tension difference decreases, which in turn results in a decrease in the intensities of capillary and gravitational motion. The result is a monotonic increase in the duration of the gravitational component of the cycle. For amyl alcohol, the effect of increasing the average concentration is much weaker. In concluding this section, we compare the critical values of the Marangoni number for the first cycle of the oscillatory regime. An increase in the number of methylene groups in an alcohol molecule from 1 to 5 leads to an increase in Ma_C^* from 0.8×10^7 to 2.4×10^7 , an increment which is very small compared to a 25-fold decrease in the critical concentration difference.

4. Laboratory simulation of Marangoni convection in microgravity

4.1 Oscillatory regimes of convective flow in a drop connected to a container

In discussing the issue of mass transfer between a drop and the liquid surrounding it, it should be noted that the case of diffusion from a free drop, which is in motion or at rest under hydroweightlessness, has been studied in the most detail. Such a drop is characterized by a rapid completion of mass transfer processes due to the absence of a constant source of the diffusing component. In addition, in a set of problems, the drop remains connected by a capillary with a large volume of the initial liquid. The existence of an additional source of the diffusing component facilitates enhancement of mass transfer and an increase in its duration. However, in most cases, the probability of such a development of events is neglected, as, for example, in the hanging drop method. The rationale for this approach is the insignificance of the diffusion flow of the soluble component from the capillary into the drop compared to its flow from the drop into the surrounding liquid. In disagreement with the generally accepted point of view are the results of an experiment that studied diffusion of surfactants from a drop under zero-gravity conditions (Foton-M satellite No. 3, 2007), according to which the flow of the initial mixture through the capillary turned out to be so intense that it formed the main flow in the drop [100].

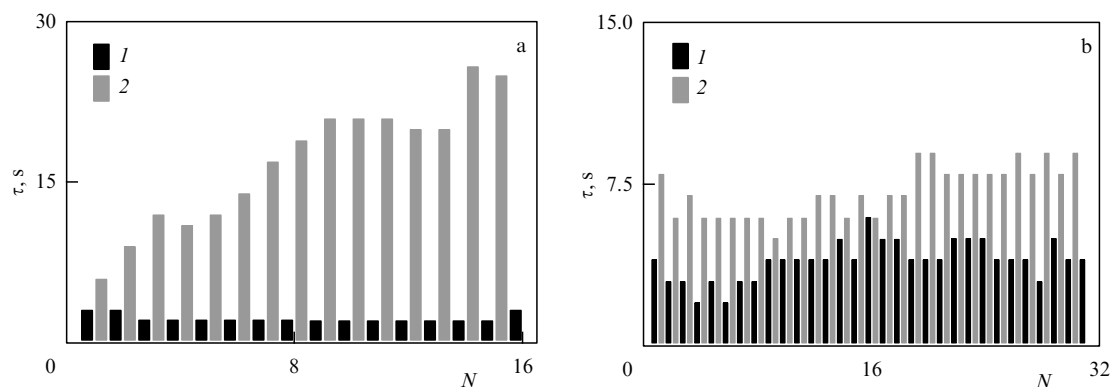


Figure 13. Existence time of capillary (1) and gravitational (2) convection vs. the number of cycles. (a) Methanol alcohol solution with $C_0 = 8\%$, $L_c = 2.0$ cm. (b) Amyl alcohol solution with $C_0 = 0.4\%$, $L_c = 0.1$ cm.

To determine the mechanism of this phenomenon, the following experiment was carried out under laboratory conditions [101]. To simulate microgravity conditions, a horizontal layer 1.2 mm thick was chosen, which forms the working cell of the Fizeau interferometer. Before the experiment, the layer was filled with water. As in the space experiment, a solution of isopropyl alcohol in chlorobenzene was used to create the drop. Water and chlorobenzene are insoluble in each other. Alcohol, on the contrary, is easily soluble in both liquids and has a lower density and a lower surface tension, thereby playing the role of a surfactant. The drop was placed in the center of the layer using a medical syringe. The inner diameter of the syringe needle was 0.64 mm, and its length was 80 mm. After its creation, the drop remained connected by a needle to a syringe, which served as a container with a volume of about $2 \times 10^3 \text{ mm}^3$ filled with the initial surfactant solution. The initial drop volume varied from 30 to 60 mm^3 . The corresponding radius of the spherical drop exceeded the thickness of the layer; therefore, during its creation, the drop was flattened and took the form of a cylinder with a free lateral boundary. The presence of flat ends made it possible to visualize the concentration field and the flow structure inside the drop.

The dissolution of drops with an initial mass concentration of alcohol C_0 ranging from 1 to 20% was studied. Figure 14 shows a series of interferograms that present the evolution of the concentration field during the diffusion of alcohol from a drop with $C_0 = 15\%$. The process was observed from the top. The countdown began at the moment when the supply of the solution during the creation of the drop was halted: at this moment, the drop attains the maximum diameter D_0 (6–8 mm). It is clearly seen that the resulting surfactant concentration field has the form of two systems of concentric fringes located inside and outside the drop. With time, the external system fringes quickly propagate from the surface of the drop into the bulk of the surrounding liquid, while the internal system fringes, on the contrary, converge to the center of the drop, where they disappear when touching each other. The total number of fringes, the rate of their emergence, and the propagation velocities are determined by the initial alcohol content. The velocity of radial displacement of the external system boundary reaches $0.2\text{--}0.3 \text{ mm s}^{-1}$, a value which is three orders of magnitude higher than the velocity of surfactant propagation due to diffusion. Consequently, the main mechanism of surfactant transport near the drop is gravitational convection, although the conditions for its suppression are in effect. Being lighter than water, alcohol, having left the

drop, floats to the upper boundary of the layer and then spreads along it. In turn, chlorobenzene, having lost alcohol, becomes heavier than the initial solution and accumulates in the lower part of the drop. As a result, a vertical gradient of surfactant concentration arises along the lateral boundary of the drop, which causes the formation of a surface tension difference and the development of capillary motion already at $C_0 \geq 2\%$. The resulting flow has the form of unsteady vortex cells, which are symmetrically located on both sides of the interface and, with increasing C_0 , engage the entire volume of the drop (Fig. 14a).

The completion of intense Marangoni convection due to a decrease in the surfactant concentration in the drop leads to the development of its diffusion from the mixture that fills the syringe needle. The surfactant, diffusing from the needle, reaches the side surface of the drop, creating a concentration gradient along it and, consequently, a surface tension gradient. The resulting capillary motion has the shape of a single large vortex (Fig. 14b) or two smaller vortices on both sides of the needle (Fig. 14c). The vortices entrain the original surfactant solution from the needle, along the axis of which a counter flow of the ‘depleted’ solution is concurrently formed from the center of the drop into the container, which arises due to the continuity of the liquid and the constancy of the container volume. With time, the vortices, increasing in size, block the cross section of the needle and mix the initial and ‘depleted’ surfactant solutions at its exit. As a result, the surfactant gradient vanishes and the Marangoni convection stops. However, the large-scale flow created in the volume of the drop decays more slowly, which leads to a new release of the surfactant from the needle and a repetition of the development cycle of capillary motion. The number of such cycles ranges from 10–20 at $C_0 = 5\%$ to 80–90 at $C_0 = 15\text{--}20\%$, while in the space experiment the Marangoni convection was quasi-stationary.

Figure 15a shows the frequency of ‘bursts’ of capillary motion during surfactant diffusion from a drop connected to a container as a function of the time when the oscillatory regime is established. It can be seen that the frequency varies over a relatively wide range only for drops with a low surfactant content. The reason is the low intensity of the capillary flow caused by the diffusion of the surfactant from the needle: most of the drop surface retains the vertical stratification of the surfactant, which plays the role of a ‘trigger’. On the contrary, for drops with high C_0 , the change in frequency with time occurs smoothly due to the fact that the capillary flow regulates the distribution of surfactants along the entire boundary of the drop. It should be noted that the average

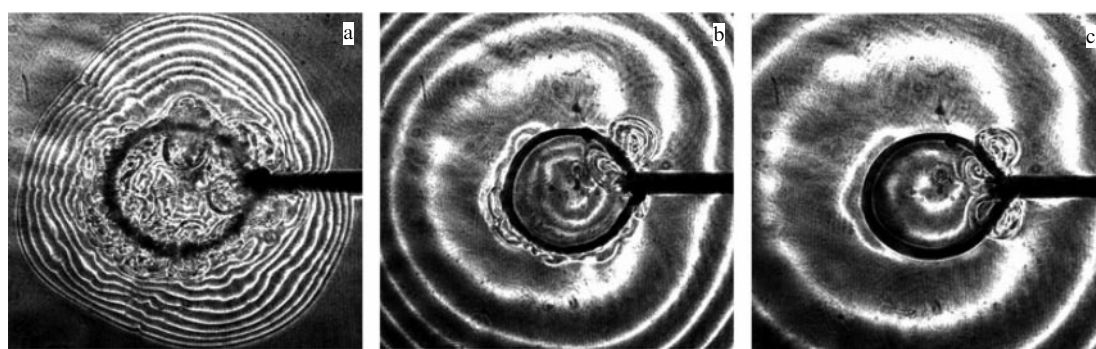


Figure 14. Evolution of the concentration field of surfactant diffusion from a drop with diameter $D_0 = 6.2 \text{ mm}$ at $C_0 = 15\%$; time from the creation of the drop: (a) $t = 8 \text{ s}$, (b) $t = 74 \text{ s}$, (c) $t = 113 \text{ s}$.

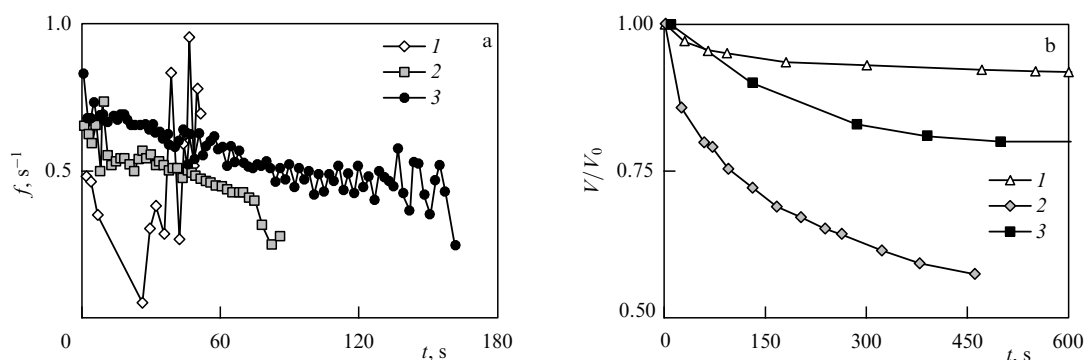


Figure 15. (a) Frequency of ‘bursts’ of capillary motion caused by surfactant diffusion from droplets as a function of the time after the onset of the oscillatory regime at $C_0 = 5\%$ (1), $C_0 = 10\%$ (2), and $C_0 = 15\%$ (3). (b) Relative volume of a drop as a function of time at $C_0 = 15\%$: 1 — a separate drop at $g = g_0$, 2 — a drop connected to a container at $g = g_0$, and 3 — a drop connected to a container under microgravity conditions.

frequency of ‘bursts’ for initial surfactant concentrations at $C_0 \geq 10\%$ remains approximately equal to 0.5 Hz, slowly decreasing, and is apparently determined by the ratio of the geometrical parameters of the needle connecting the drop and the container (in particular, the diameter of the needle determines the volume of the surfactant supplied to the drop).

Figure 15b shows the change in the relative volume of a drop during surfactant diffusion for various levels of gravity. The comparison shows that the maximum reduction in volume is achieved under terrestrial conditions for a drop connected to a container (curve 2). The reason for this is the leading role of free convection in maintaining the surfactant gradient normal to the drop boundary due to the creation of an advective flow in the environment. If the initial and final volumes of the drop and the initial concentration of alcohol in the drop are known, then, using the dependence of the contraction of the chlorobenzene solution of alcohol on the concentration of the latter, it is possible to estimate the volume of the initial surfactant solution involved in mass transfer. In particular, at $C_0 = 15\%$, the volume of such a surfactant solution can be up to two initial volumes of the drop. It should be noted that, under microgravity conditions ($g \sim 10^{-4}g_0$), the intensity of mass transfer between the drop and the container noticeably decreases (curve 3).

Thus, laboratory modeling of surfactant diffusion makes it possible to explain the unexpectedly strong decrease in the volume of a drop in a space experiment and to reveal the mechanism which forms the main flow in it. It has been shown that free convection, despite the conditions for its maximum suppression being created, still affects to a significant extent the mass transfer between the drop and the environment. In addition, the data obtained suggest a new insight into the results of studying the dynamics of changes in surface tension in systems of liquids, one of the components of which can exhibit surface-active properties, as is established using the hanging drop method.

4.2 Simulation of Marangoni instability for homogeneous diffusion of surfactants through an interface under zero-gravity conditions

The main problem with laboratory modeling of hydrodynamic processes in zero-gravity conditions is that the effect of gravity cannot be completely removed. Conventionally, modeling is carried out using the Grashof number Gr_C . In this case, a change in two parameters is used: $\Delta\rho$ (in hydrostatic problems) and h (in convective problems).

Diminishing h makes it possible to effectively reduce the intensity of gravitational convection while maintaining unchanged all the physical and chemical properties of the medium. However, in the experiment, a decrease in the value of Gr_C by means of a decrease in the vertical size of the cavity is only possible up to a certain limit set by both the resolution of the experimental setup and the need to maintain the ratio of the areas of predominance of gravitational and capillary (or due to another mechanism alternative to gravity) convection. If this ratio is changed, simulation is no longer adequate.

In problems of diffusion in a system of immiscible liquids, an additional approach to reducing the Grashof number is available: the initial levelling of the densities of the base liquids on both sides of the interface in terms of the density of the diffusing component. In this case, all further density variations are mainly associated with the contraction effect, the essence of which is a nonadditive change in the volume of the mixture as a result of absorption or diffusion of one of its components. The reason for the contraction is the dependence of the average distance between the molecules of the mixture components on their concentration. Estimates show that the density differences arising due to contraction can reach a value sufficient to initiate free convection; however, most often they are approximately an order of magnitude smaller than in the case of diffusion in a system with an arbitrary density of base liquids.

To test this approach, experiment [102] studied the development of convection resulting from the diffusion of surfactants in a system of liquids with initially equal densities and with a vertical interface blocking the horizontal channel. The base (contacting) liquids were an aqueous solution of sodium chloride (base liquid 1) and a mixture of benzene and chlorobenzene (base liquid 2). The initial densities of the base liquids were equal to the density of the diffusing component, the role of which was played by acetic acid. Initially, the acid was concentrated in a binary mixture. The density of acetic acid at a temperature of 25°C is 1.042 g ml^{-1} [80]. To attain the same density, the mass concentration of benzene in its mixture with chlorobenzene was increased to $C_{01} = 21\%$. The concentration of sodium chloride in water $C_{02} = 7.2\%$. A cell with a rectangular cavity 26 mm high, 1.4 mm wide, and 75 mm long was chosen for the experiments. Parallel glass liners in the cavity formed a horizontal channel 2.6 mm high, 1.4 mm wide, and 36 mm long. The left end of the channel adjoined the side wall of the cavity, while the right end of the channel was open (and, consequently, connected to the cavity). The cell had a

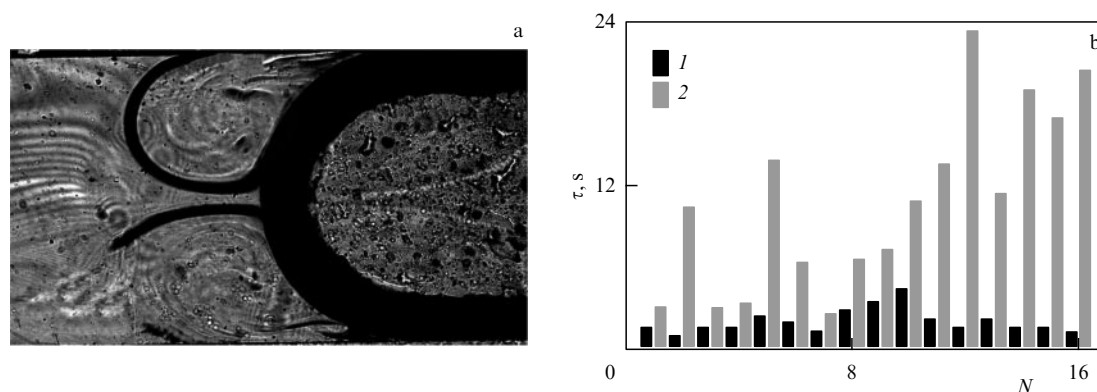


Figure 16. (a) Structure of the concentration field near the interface at $C_0 = 20\%$, the time from the beginning of the Marangoni convection cycle is 3 s, the time of the beginning of the cycle from the moment the drop is created is $t = 29$ s. (b) Dependence of the lifetimes at $C_0 = 20\%$ of capillary (1) and gravitational (2) convection on the number of cycles N .

number of holes intended for filling and draining liquids and for installing a movable vertical partition.

All experiments were carried out according to the following procedure. Initially, the channel was divided into two parts using a partition. A mixture of benzenes containing acetic acid was introduced into the left side of the channel through a tube. The right part of the channel and the remaining part of the cavity were filled with an aqueous salt solution; the partition was then removed, and the process of acid diffusion began, the dynamics of which were monitored in real time by an interferometer. Due to the contraction, the diffusion of the acid was accompanied by an increase in the density of both contacting liquids. Further development of the process depended on the initial acid concentration in the drop. At subthreshold acid concentrations ($C_0 \leq 10\%$), there was no capillary motion. In this case, the ‘depleted’ mixture on the left and the aqueous solution ‘enriched’ in acid on the right of the interface flowed down along the interface and then spread in the form of ‘tongues’ along the bottom of the channel.

At a C_0 value exceeding the threshold value for the development of Marangoni convection, the flow pattern changed sharply (Fig. 16). The emerging vortex capillary motion encompassed a significant part of the channel, destroying the concentration distribution formed by diffusion. The competition between the intense capillary flow, leveling the inhomogeneous distribution of concentration along the interface, and the slow advective flow, restoring the vertical difference in concentration along it, resulted in the onset of an oscillatory regime of concentration convection. The generated flow had the form of two paired vortices (Fig. 16a), the structure of which corresponds to that of convective motion at the initial stage in the numerical experiment for zero-gravity conditions. A similar system of vortices was obtained in the model with the surface phase of the surfactant when the coefficients of adsorption and desorption of base liquid 1 exceeded those of base liquid 2.

Immediately after the completion of the first ‘burst’ of capillary motion, a vertical distribution of density (and acid concentration) of base liquids was established in the main part of the channel. As a result, the upper vortex of the next ‘burst’ of Marangoni convection developed in a mixture with a higher acid content than the lower one and was characterized by both a greater intensity of movement and a higher rate of mass flow through the interface. The intensity of the latter

process is so high that the acid concentration gradient between the vortex and the rest of the volume mixture was visually perceived as an interface between phases. The lower vortex largely emerged due to viscous friction.

Figure 16b displays a diagram of the change in the times of dominance of capillary and gravitational convection in various cycles of the oscillatory regime. As can be seen from the figure, the duration of the cycles is not a regular function. However, the trend of increasing the duration of the cycle with an increase in the number of oscillations is clearly visible. As in most of the situations discussed above, the cycle duration increases due to an increase in the time needed for the acid concentration difference at the interface to be restored by the advective flow.

In conclusion, we note that in this problem the oscillatory regime develops due to the diffusion of surfactants from an initially homogeneous mixture into an initially homogeneous solution. The reason for the emergence of capillary convection is the large characteristic diffusion times and the action of gravity, which leads to the formation of a vertical stratification of the surfactant near the boundary. Undoubtedly, the onset of the oscillatory regime is also facilitated by the impossibility of a solution ‘enriched’ in acid to leave the vicinity of the drop. It is clear that the duration of such a regime of oscillations is short, since it is limited by the surfactant content in the drop. In this case, as before, the oscillatory mode of surfactant mass transfer switches to the diffusion mode long before the acid in the drop is fully depleted due to the presence of surface-active impurities at the interface. Measurements show that approximately 9% of the acid is retained in the drop at the corresponding moment of time, a value slightly below the threshold ($\sim 10\%$) for the development of capillary motion.

5. Conclusions

We have made an attempt to represent the most interesting and significant experimental work and show that the use of optical methods makes it possible to advance from a qualitative description of oscillatory modes to quantitative measurements. Visualization of the surfactant concentration fields and the flow structure enabled the determination of the period of oscillations and the duration of the oscillatory regime as functions of the parameters of the surfactant concentration distribution, the physicochemical properties

of the contacting liquids, the surfactants employed in the experiment, and their surface activity. The development of oscillatory flow regimes near bubbles and drops in vertical and horizontal layers and near a vertical interface has been analyzed. It is confirmed that the reason for the establishment of oscillatory regimes is driven by competition between the capillary and gravitational mechanisms of motion of liquids with significantly different characteristic times. For the behavior of systems of liquids with an interface and a nonequilibrium distribution of soluble surfactants, the ratio of chemical potentials, which determine the direction of surfactant diffusion and the dynamics of adsorption-desorption processes, is of great importance. It is shown that uncontrolled surface-active impurities play an important role in the onset of the oscillatory regime, setting the conditions for its development and change and leveling its duration and period in each cycle.

Undoubtedly, studies of such flow regimes in liquid systems with an interface are of great interest for hydrodynamics, mass transfer, and the physics of chemical processes. In essence, such problems are a testing ground for developing theoretical models and methods for numerical calculations of heat and mass transfer through a phase boundary with consideration for adsorption-desorption processes under capillary motion and the diffusion/gravitational mechanism for maintaining the composition of liquids near the surface.

Unexpected, at first glance, may be the extension of the results obtained in the study of oscillatory regimes to biology. For example, the search in inanimate nature for analogs of the functions of unicellular organisms, for example, movement (an analog is the capillary drift of drops), leads to a comparison of the functions of nutrition and excretion of waste products, on the one hand, and absorption and extraction of excess surfactant by a drop located in its inhomogeneous solution, on the other hand. Due to the fact that the volume of liquid entrained by the advective flow is much larger than that of a drop, the latter can be considered a concentrator of organic microimpurities that can be used later as a building material for high-molecular compounds. Finally, the ability of an ensemble of drops to synchronize their oscillations and transmit a perturbation of the concentration field over a considerable distance can be considered an element of group behavior [103, 104].

Involvement of Marangoni convection leads to the enhancement of mass transfer processes in multiphase media. When the threshold concentration of a surfactant is reached, any motionless bubble or drop is transformed into a kind of *perpetuum mobile* for mixing inhomogeneous liquids and extraction (in the case of a drop), which does not require any mechanical parts and is therefore very promising for microfluidic technologies applied in the chemical and pharmaceutical industries [105]. A special role can be played by the detected effects in the creation of microsystems for cooling and heat exchange using multi-component mixtures of liquids as a coolant. A new direction might be the development of dispensers based on drops connected to a container. Studies of oscillatory regimes near vertical interfaces offer new options for enhancing mass transfer processes that involve porous media and perforated surfaces.

This study was financially supported by the Russian Foundation for Basic Research as part of research project no. 20-11-50086_., Expansion.

References

- Landau L D, Lifshitz E M *Fluid Mechanics* (Oxford: Pergamon Press, 1987); Translated from Russian: *Gidrodinamika* (Moscow: Nauka, 1988)
- Myshkis A D (Ed.) *Low-Gravity Fluid Mechanics* (Berlin: Springer-Verlag, 1987); Translated from Russian: *Gidrodinamika Nevesomosti* (Moscow: Nauka, 1976)
- Levich V G *Physicochemical Hydrodynamics* (Englewood Cliffs, NJ: Prentice-Hall, 1962); Translated from Russian: *Fiziko-Khimicheskaya Gidrodinamika* (Moscow: GIFML, 1959)
- Varley C R. *Soc. Arts Sci. Mauritius* **50** 190 (1836)
- Weber E H *Ber. Verhandl. Kon. Sachs. Ges. Wiss. Leipzig* (1854)
- Thomson J *Philos. Mag.* **10** 330 (1855)
- Segner J A *Comment. Soc. Reg. Götting.* (1751)
- Marangoni C G M *Sull'espansione dell goccie di un liquido galleggiante sulla superficie di altro liquido* (Pavia: Tipografia Fusi, 1865)
- Van der Mensbrugghe G *Mem. Couronnees Mem. Savants etrangers* **34** (1) 1 (1870)
- Van der Mensbrugghe G *Mem. Couronnees Mem. Savants etrangers* **37** (4) 1 (1873)
- Marangoni C G M *Nuovo Cimento* **2** 3 105 (1870)
- Marangoni C G M *Ann. Physik Chem.* **143** 337 (1871)
- Plateau J A F *Statique expérimentale et théorique des liquides soumis aux seules forces moléculaires* (Paris: Gauthier-Villars, 1873)
- Dupré de Rennes A *Théorie Mécanique de la Chaleur* (Paris: Gauthier-Villars, 1869)
- Young C *Philos. Trans. R. Soc. London* **95** 65 (1805)
- Laplace P S *Traité de mécanique céleste; supplément au dixième livre, sur l'action capillaire* (Paris: Courcier, 1806)
- Maxwell J C *Theory of Heat* (London: Longmans, Green and Co., 1871)
- Maxwell J C, in *Encyclopedia Britannica* 9th ed., Vol. 5 (Edinburgh: Adam and Clark, 1878)
- Harkins W D, Feldman A J. *Am. Chem. Soc.* **44** 2665 (1922)
- Gibbs J W *Trans. Conn. Acad.* **3** (1878)
- Gibbs J W *The Collected Works* Vol. 1 (New Haven, CT: Yale Univ. Press, 1948; *Statisticheskaya Fizika* (Moscow: Nauka, 1982)
- Frumkin A *Nature* **7** 235 (1928)
- Rice J A *Commentary of the Scientific Writings of J.W. Gibbs* (New Haven, 1936)
- Buff F P J *J. Chem. Phys.* **19** 1591 (1951)
- Kondo S J *J. Chem. Phys.* **25** 662 (1956)
- Rebinder P A *Poverkhnostnye Yavleniya v Dispersnykh Sistemakh. Kolloidnaya Khimiya. Izbrannye Trudy* (Surface Phenomena in Disperse Systems. Colloid Chemistry. Selected Works) (Moscow: Nauka, 1978)
- Rusanov A I *Termodinamika Poverkhnostnykh Yavlenii* (Thermodynamics of Surface Phenomena) (Leningrad: Izd. LGU, 1960)
- Rusanov A I *Fazovye Ravnovesiya i Poverkhnostnye Yavleniya* (Phase Equilibria and Surface Phenomena) (Leningrad: Khimiya, 1967)
- Lewis J B, Pratt H R C *Nature* **171** 1155 (1953)
- Sterling V, Scriven L E *AIChE J.* **5** 514 (1959)
- Scriven L E *Chem. Eng. Sci.* **12** (4) 98 (1960)
- Young N O, Goldstein J S, Block M J *J. Fluid Mech.* **6** 350 (1959)
- Povitskii A S, Lyubin L Ya *Osnovy Dinamiki i Teploobmena Zhidkostei i Gazov pri Nevesomosti* (Basics of the Dynamics and Heat Exchange of Fluids and Gases at Zero Gravity) (Moscow: Mashinostroenie, 1972)
- Ganiev R F, Lapchinskii V F *Problemy Mekhaniki v Kosmicheskoi Tekhnologii* (Mechanical Problems in Space Technology) (Moscow: Mashinostroenie, 1978)
- Avduesvskii V S et al. *Problemy Kosmicheskogo Proizvodstva* (Space Manufacturing Problems) (Moscow: Mashinostroenie, 1980)
- Grishin S D, Leskov L V *Industrializatsiya Kosmosa* (Industrialization of Space) (Moscow: Nauka, 1987)
- Walter H U (Ed.) *Fluid Sciences and Materials Science in Space* (Berlin: Springer-Verlag, 1987)
- Ratke L, Walter H, Feuerbacher B (Eds) *Materials and Fluids under Low Gravity* (Berlin: Springer-Verlag, 1989)
- Pukhnachov V V *Fluid Dynamics Trans.* **14** 145 (1989)

40. Rath H J (Ed.) *Microgravity Fluid Mechanics* (Berlin: Springer-Verlag, 1991)
41. Monti R (Ed.) *Physics of Fluids in Microgravity* (London: Taylor and Francis, 2001)
42. Subramanian R S, Balasubramanian R *The Motion of Bubbles and Drops in Reduced Gravity* (Cambridge: Cambridge Univ. Press, 2001)
43. Birikh R V et al. *Liquid Interfacial Systems: Oscillations and Instability* (New York: M. Dekker, 2003)
44. Starov V M, Velarde M G, Radke C J *Surfactant Science Series* Vol. 138 (London: Taylor and Francis, 2007)
45. Bratukhin Yu K *Ravnovesie i Ustoichivost' Geterogennykh Sistem* (Equilibrium and Stability of Heterogeneous Systems) (Perm: Izd. Perm. Univ., 1987)
46. Bratukhin Yu K, Makarov S O *Mezhfaznaya Konveksiya* (Interfacial Convection) (Perm: Izd. Perm. Univ., 1994)
47. Bratukhin Yu K, Makarov S O *Gidrodinamicheskaya Ustoichivost' Mezhfaznykh Poverkhnostei* (Hydrodynamic Stability of Interfaces) (Perm: Izd. Perm. Univ., 2005)
48. Zuev A L, Kostarev K G *Dokl. Phys.* **49** 747 (2004); *Dokl. Ross. Akad. Nauk* **399** 490 (2004)
49. Bratukhin Yu K et al. *Exp. Fluids* **38** 594 (2005)
50. Jehring H, Viet Huyen N, Horn E J. *Electroanal. Chem.* **88** (2) 265 (1978)
51. Wang M, Ming N *Phys. Rev. A* **44** 7898 (1991)
52. Stoilov Y Yu *Langmuir* **14** 5685 (1998)
53. Stoilov Yu Yu *Phys. Usp.* **43** 39 (2000); *Usp. Fiz. Nauk* **170** 41 (2000)
54. Startsev A V, Stoilov Yu Yu *Quantum Electron.* **32** 463 (2002); *Kvantovaya Elektron.* **32** 463 (2002)
55. Bratukhin Yu K et al. *Izv. Ross. Akad. Nauk. Mekh. Zhidk. Gaza* (3) 11 (2009)
56. Ashurov M et al. *J. Phys. Conf. Ser.* **1124** 051008 (2018)
57. Raake D, Siekmann J, Chun Ch-H *Exp. Fluids* **7** 164 (1989)
58. Wozniak K, Wozniak G, Rösgen T *Exp. Fluids* **10** 12 (1990)
59. Chun C H, Raake D, Hansmann G *Exp. Fluids* **11** 359 (1991)
60. Rashidnia N, Balasubramanian R *Exp. Fluids* **11** 167 (1991)
61. Kassemi M, Rashidnia N *Phys. Fluids* **10** 3133 (2000)
62. Arlabosse P et al. *Heat Transfer* **122** (1) 66 (2000)
63. Betz J, Straub J *Heat Mass Transfer* **37** 215 (2001)
64. Wozniak G et al. *Exp. Fluids* **31** 84 (2001)
65. Reynard C, Santini R, Tadrist L *Heat Transfer* **122** 66 (2001)
66. Chun C-H, Raake D, Hansmann G *Exp. Fluids* **11** 359 (1991)
67. Betz J, Straub J *Heat Mass Transfer* **37** 215 (2001)
68. Reynard C, Santini R, Tadrist L *C.R. Mechanique* **331** (3) 237 (2003)
69. Mizev A I *Priklad. Mekh. Tekh. Fiz.* **45** (5) 102 (2004)
70. Dupeyrat M, Nakache E *Bioelectrochem. Bioenerget.* **5** 134 (1978)
71. Kovalchuk N M, Vollhardt D *Adv. Colloid Interface Sci.* **120** (1–3) 1 (2006)
72. Kovalchuk N M et al. *Langmuir* **28** 6893 (2012)
73. Mizev A, Birikh R *Eur. Phys. J. Spec. Top.* **192** (1) 145 (2011)
74. Schwarzenberger S, Eckert K, Odenbach S *Chem. Eng. Sci.* **68** 530 (2012)
75. Zuev A L, Kostarev K G *Phys. Usp.* **51** 1027 (2008); *Usp. Fiz. Nauk* **178** 1065 (2008)
76. Kostarev K G, Zuev A L, Viviani A *C.R. Mecanique* **332** (1) 1 (2004)
77. Kostarev K G, Zuev A L, Viviani A *Appl. Mech. Trans. ASME* **73** (1) 66 (2006)
78. Zuev A L, Kostarev K G *J. Exp. Theor. Phys.* **103** 317 (2006); *Zh. Eksp. Teor. Fiz.* **130** 363 (2006)
79. Vazquez G, Alvarez E, Navaza J M *J. Chem. Eng. Data* **40** 611 (1995)
80. Nikol'skii B P (Ed.) *Spravochnik Khimika* (Chemist's Reference Book) Vol. 3 (Leningrad: Khimiya, 1962)
81. Schott R, Pfennig A *Mol. Phys.* **102** 331 (2004)
82. Kostarev K G, Briskman V A *Dokl. Phys.* **46** 349 (2001); *Dokl. Ross. Akad. Nauk* **378** 187 (2001)
83. Kostarev K G et al. *Int. J. Micrograv. Sci. Technol.* **19** (2) 26 (2007)
84. Kim M et al. *Eur. Phys. J. Spec. Top.* **192** 185 (2011)
85. Schwarzenberger K et al. *Colloids Surf. A* **481** 633 (2015)
86. Birikh R V et al. *Izv. Ross. Akad. Nauk. Mekh. Zhidk. Gaza* (4) 30 (2006); *Fluid Dyn.* **41** 514 (2006)
87. Kostarev K G, Zuev A L, Viviani A *Int. J. Micrograv. Sci. Technol.* **21** 59 (2009)
88. Bushueva K A et al. *Colloid J.* **70** 416 (2008); *Kolloid. Zh.* **70** 457 (2008)
89. Kostarev K G, Zuev A L, Viviani A *Acta Astronautica* **62** 431 (2008)
90. Gorodetskaya A V *Zh. Fiz. Khim.* **23** (1) 71 (1949)
91. Denisova M O “Nestatsionarnaya kontsentratsionnaya konveksiya Marangoni v vertikal'nykh sloyakh zhidkosti” (“Non-stationary Marangoni concentration convection in vertical layers of liquid”), PhD Thesis (Phys.-Math. Sci.) (Perm: Institute of Continuous Media Mechanics of the Ural Branch of Russian Academy of Science, 2013)
92. Birikh R V, Rudakov R N *Vychisl. Mekh. Splosh. Sred* **3** (1) 24 (2010)
93. Birikh R V *Vestn. Nizhegorod. Univ. im. N I Lobachevskogo* (4–3) 647 (2011)
94. Birikh R V, Denisova M O, Kostarev K G *Izv. Ross. Akad. Nauk. Mekh. Zhidk. Gaza* (6) 56 (2011); *Fluid Dyn.* **46** 890 (2011)
95. Birikh R V, Pukhnachev V V, Frolovskaya O A *Izv. Ross. Akad. Nauk. Mekh. Zhidk. Gaza* (1) 192 (2015); *Fluid Dyn.* **50** 173 (2015)
96. Shmyrov A, Mizev A *Langmuir* **35** 14180 (2019)
97. Duclaux E *Ann. Chim. Phys.* **13** (5) 76 (1878)
98. Traube I *Liebigs Ann. B* **265** (1) 27 (1891)
99. Denisova M O, Kostarev K G *Procedia IUTAM* **8** 75 (2013)
100. Kostarev K G et al. *Acta Astronautica* **66** (3–4) 427 (2010)
101. Denisova M O, Kostarev K G, Shmyrov A V *Micrograv. Sci. Technol.* **30** (4) 353 (2018)
102. Birikh R V, Denisova M O, Kostarev K G *J. Appl. Mech. Tech. Phys.* **60** 1264 (2019); *Vychisl. Mekh. Splosh. Sred* **11** (4) 463 (2018)
103. Eckert K et al. *Soft Matter* **14** 9250 (2018)
104. Čejkova J et al. *Colloids Surf. A* **566** 141 (2019)
105. Bratsun D et al. *Micromachines* **9** 600 (2018)